

SECOND-ORDER RAYLEIGH-SCHRÖDINGER PERTURBATION THEORY FOR THE GRASP2018 PACKAGE: VALENCE-VALENCE CORRELATIONS

G. Gaigalas, P. Rynkun, and L. Kitovienė

Institute of Theoretical Physics and Astronomy, Faculty of Physics, Vilnius University, Saulėtekio 3, 10257 Vilnius, Lithuania
Email: gediminas.gaigalas@tfai.vu.lt; pavel.rynkun@tfai.vu.lt; laima.radziute@tfai.vu.lt

Received 22 November 2024; accepted 2 December 2024

The accurate description of electron correlations remains a major challenge in atomic calculations. In order to perform accurate calculations, it is necessary to consider various types of electron correlations and this often leads to extensive configuration state function (CSF) expansions. This work presents further development of the method based on the second-order perturbation theory to identify the most significant CSFs that have the greatest influence on core-valence, core, core-core and valence-valence correlations. This method is based on a combination of the relativistic configuration interaction method and the stationary second-order Rayleigh-Schrödinger many-body perturbation theory in an irreducible tensorial form [G. Gaigalas, P. Rynkun, and L. Kitovienė, Second-order Rayleigh-Schrödinger perturbation theory for the GRASP2018 package: core-valence correlations, *Lith. J. Phys.* **64**(1), 20–39 (2024), <https://doi.org/10.3952/physics.2024.64.1.3>, G. Gaigalas, P. Rynkun, and L. Kitovienė, Second-order Rayleigh-Schrödinger perturbation theory for the GRASP2018 package: core correlations, *Lit. J. Phys.* **64**(2), 73–81 (2024), <https://doi.org/10.3952/physics.2024.64.2.1>, and G. Gaigalas, P. Rynkun, and L. Kitovienė, Second-order Rayleigh-Schrödinger perturbation theory for the GRASP2018 package: core-core correlations, *Lith. J. Phys.* **64**(3), 139–161 (2024), <https://doi.org/10.3952/physics.2024.64.3.1>]. The method is extended to include additionally valence-valence electron correlations. It can be applied for an atom or ion with any number of valence electrons for the calculation of energy spectra and other properties. Meanwhile, the correlations which cannot be included according to perturbation theory are taken into account in a regular way. The use of the developed method allows a significant reduction of CSFs especially for complex atoms and ions. As an example of its application, the atomic calculations of the energy structure for Se III ion are presented.

Keywords: configuration interaction, spin-angular integration, perturbation theory, tensorial algebra, valence-valence correlations, core-valence correlations, core correlations, core-core correlations

1. Introduction

The accurate calculation of atomic properties requires correlation and relativistic effects to be taken into account as much as possible. The General Relativistic Atomic Structure (GRASP) software package [1, 2] is currently one of the most widely used software packages for such problems in atomic theory. It is well developed and has various options for capturing correlation effects as accurately as possible. But currently, the demand for the accuracy of atomic quantities is very high, therefore the development of further methods and their implementation in software is needed. This series of

papers [3–5] (the present paper included) aim to develop a method that builds on the conventional methods [6] already implemented in the GRASP software package and, in addition, takes further advantage of perturbation theory (PT) [7, 8].

Brillouin-Wigner perturbation theory (zero-first-order method) [6, 7, 9–11] has been used (without an energy iterative procedure) in the GRASP software package for a number of years. This latter version of the perturbation theory has a number of advantages (Ref. [8], Subsection 1.3.3.1) over its other version, the Rayleigh-Schrödinger perturbation theory: (i) Rayleigh-Schrödinger theory can be regarded as an approximation to

Brillouin–Wigner theory; (ii) Brillouin–Wigner theory is formally much simpler than the Rayleigh–Schrödinger theory; (iii) the convergence of Brillouin–Wigner perturbation theory is often more rapid than that of Rayleigh–Schrödinger theory for a given problem; (iv) Brillouin–Wigner perturbation theory may converge for problems for which Rayleigh–Schrödinger theory does not; (v) Brillouin–Wigner perturbation theory is often more convenient to use for degenerate problems. It also has the disadvantages of Brillouin–Wigner theory against Rayleigh–Schrödinger perturbation theory (Ref. [8], Subsection 1.3.3.2): (i) Brillouin–Wigner perturbation theory is iterative, since the exact energy is contained in the denominators arising in the expressions for the energy components; (ii) Brillouin–Wigner perturbation theory is not explicitly a many-body theory, in that the energy expressions in each order do not scale linearly with a particle number.

The summary of Rayleigh–Schrödinger many-body perturbation theory (RSMBPT) was given in the 1990s [7]. It was then developed in the framework of non-relativistic atomic theory, using determinants. Although this theory has some weaknesses, its strengths stimulate further development of the theory. Its further modification resulted in an irreducible tensorial form of effective Hamiltonian in the first two orders of PT [12–14]. The spin-angular part of Feynman diagrams in this version of theory is represented by the sum of irreducible tensorial products, composed of two, four and six creation and annihilation operators, which correspond to the Feynman diagrams with two, four and six free lines [14]. This allows one to use the Racah algebra [15–19] including the quasispin [20, 21] for spin-angular integration in the *LS*-coupling [22]. But both the Rayleigh–Schrödinger perturbation theory [7] and the irreducible tensorial form of this theory [12–14] are not suitable for use in the GRASP software package: (a) GRASP is based on relativistic atomic theory [23, 6], and Rayleigh–Schrödinger perturbation theory [7, 12–14] is based on non-relativistic atomic theory; (b) the single electron orbitals in the GRASP software package are searched for in an arbitrary potential (in multiconfiguration Dirac–Hartree–Fock approximation [23]), which in the most general case does not satisfy the requirements of Rayleigh–Schrödinger many-

body perturbation theory [7]. The latter problem (b) was successfully solved [24, 25] by applying the theory in a non-relativistic framework of atomic theory using a superposition of the configurations approach [26], where the SAI software library [27] was used to search for the spin-angular coefficients in the *LS*-coupling [22]. This series of articles [3–5] (including this one) is the final stage of development of this theory, i.e. both problems (a) and (b) are successfully solved at once. This means that RSMBPT theory is finally developed in such a way that it can easily be used in the GRASP software package.

In fact, the method developed in this paper is a combination of the relativistic configuration interaction (RCI) method and RSMBPT theory in an irreducible tensorial form (RCI (RSMBPT)), where core–valence (CV), core (C), core–core (CC) and valence–valence (VV) correlations are included according to the stationary second-order Rayleigh–Schrödinger many-body perturbation theory. It no longer suffers from disadvantage (ii) (see Ref. [8], Subsection 1.3.3.1), since the theory is implemented in the GRASP software package [1, 2] and the user simply uses it as a ‘black box’, inputting only the data of the system (atom or ion) under consideration. The remaining drawbacks (i), (iii), (iv) and (v) (see Ref. [8], Subsection 1.3.3.1) are also no longer relevant in the methodology proposed in this paper, as a number of correlation effects are included in the framework of the multiconfiguration Dirac–Hartree–Fock approximation [23, 28] already in the zero order of perturbation theory. Moreover, it is used in such a way that the methodology is not used for the final calculations, but rather for the assessment of the influence of correlations – which correlations have the largest contribution to the final results, and which correlations need to be included in the final RCI calculations. In addition, the methodology proposed in this work, RCI (RSMBPT), also without restrictions, allows the use of Brillouin–Wigner theory (zero-first-order method without an energy iterative procedure) [6, 7, 9–11], which is already implemented in the GRASP software package [1, 2]. So now, the (i)–(v) disadvantages of the Rayleigh–Schrödinger perturbation theory listed in Ref. [8], Subsection 1.3.3.1 are removed and only the (i) and (ii) advantages from Ref. [8], Subsection 1.3.3.2 remain.

All the expressions for the Feynman diagrams corresponding to the valence–valence correlations in relativistic atomic theory are first presented in Section 2. The modified expressions of the Feynman diagrams, which are able to use the spin-angular program library `librang` [29] from GRASP [1, 2] with any further modifications, are given in Section 3. The validity and efficiency of the presented RCI (RSMBPT) method is demonstrated in Section 4, where the energy spectrum of the Se III ion is theoretically studied.

2. Relativistic second-order effective

Hamiltonian of an atom or ion in an irreducible tensorial form for valence–valence correlations

New Feynman diagrams are used to describe valence–valence correlations, which were not available for core–valence, core and core–core correlations. We discuss this in detail below.

2.1. The first type of valence–valence correlations

This type of valence–valence correlations is presented through the Feynman diagrams VV_1 from Fig. 1 and VV_2 from Fig. 2, where all lines with a double arrow of diagrams are renamed m , i.e. $m' = n = n' \equiv m$:

$$(n_m \ell_m) j_m^{w_m} (n_n \ell_n) j_n^{w_n} \rightarrow \\ \rightarrow (n_m \ell_m) j_m^{w_m-2} (n_n \ell_n) j_n^{w_n} (n_r \ell_r) j_r (n_s \ell_s) j_s, \quad (1)$$

$$(n_m \ell_m) j_m^{w_m} (n_n \ell_n) j_n^{w_n} \rightarrow \\ \rightarrow (n_m \ell_m) j_m^{w_m-2} (n_n \ell_n) j_n^{w_n} (n_s \ell_s) j_s^2. \quad (2)$$

Each second-order Feynman diagram's expression of Rayleigh–Schrödinger many-body perturbation theory as mentioned in Refs. [3–5] has the energy denominator $D = \sum (\varepsilon_{\text{down}} - \varepsilon_{\text{up}})$, where $\varepsilon_{\text{down}}$ (ε_{up}) is the single-particle eigenvalue associated with the down- (up-) orbital lines to (from) the lowest interaction line of the diagram. For example, the denominators for the VV_1 diagram are

$$D = (\varepsilon_{m'} + \varepsilon_n - \varepsilon_r - \varepsilon_s), \quad (3)$$

where the indexes m' and n belong to the F' set, and r, s belong to the G set of orbitals [3].

Also, the following notations are used in the expressions of these diagrams (see Figs. 1 and 2):

$$X_k(ij, i'j') = \\ = \langle \ell_i j_i || C^{(k)} || \ell_{i'} j_{i'} \rangle \langle \ell_j j_j || C^{(k)} || \ell_{j'} j_{j'} \rangle R^k(n_i j_i n_{j'} j_{j'}) (4)$$

where $R^k(n_i j_i n_{j'} j_{j'})$ is the radial integral of electrostatic interaction between electrons (Ref. [28], Eqs. (89) and (90)), and $\langle \ell_i j_i || C^{(k)} || \ell_{i'} j_{i'} \rangle$ is the reduced matrix element of the irreducible tensor operator $C^{(k)}$ in the jj -coupling.

Depending on how the Feynman diagrams VV_1 and VV_2 act on the open subshells (orbitals from the F' set), the operators of the second quantization (open lines with a double arrow in the diagrams) take on the corresponding values, i.e. specific values for the summation parameters m, m', n and n' . In addition, in the diagram VV_1 , the summation parameter n passes through all possible orbitals that belong to the F' set. All these specific values of the parameters m, m', n and n' determine the type of valence–valence correlations

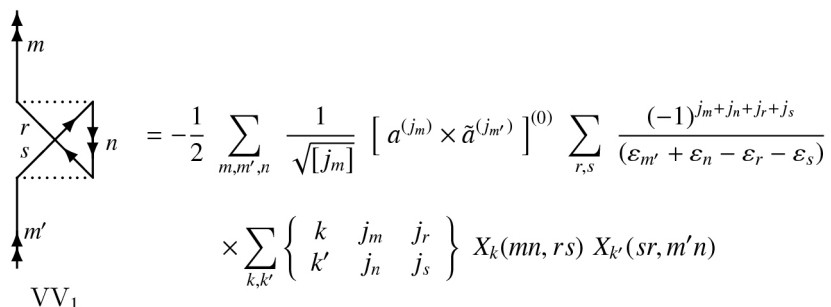


Fig. 1. The VV one-particle Feynman diagram of the second-order effective Hamiltonian for valence–valence correlations.

$$\begin{aligned}
 & m \uparrow \quad n \uparrow \\
 & \dots \dots \dots \dots \\
 & m' \downarrow \quad n' \downarrow \\
 & VV_2 = \frac{1}{2} \sum_{m,m'} \sum_{n,n'} \sum_{j_{12}} \sqrt{j_{12}} \left[[a^{(j_m)} \times \tilde{a}^{(j_{m'})}]^{(j_{12})} \times [a^{(j_n)} \times \tilde{a}^{(j_{n'})}]^{(j_{12})} \right]^{(0)} \\
 & \times \sum_{r,s} \sum_{k,k'} \frac{(-1)^{j_m + j_{m'} + j_n + j_{n'}}}{(\varepsilon_{m'} + \varepsilon_{n'} - \varepsilon_r - \varepsilon_s)} \left\{ \begin{array}{ccc} k & k' & j_{12} \\ j_{m'} & j_m & j_r \end{array} \right\} \left\{ \begin{array}{ccc} k & k' & j_{12} \\ j_{n'} & j_n & j_s \end{array} \right\} \\
 & \times X_k(mn, rs) X_{k'}(rs, m'n')
 \end{aligned}$$

Fig. 2. The VV two-particle Feynman diagram of the second-order effective Hamiltonian for valence–valence correlations.

represented by the Feynman diagrams. We also note that in the algebraic expressions of the both diagrams VV_1 and VV_2 , the sum over the excited orbits $n_r \ell_r j_r$ and $n_s \ell_s j_s$ runs.

The diagram VV_1 is a one-particle Feynman diagram, where its tensorial part is expressed through the tensorial product of creation $a^{(j)}$ and annihilation $\tilde{a}^{(j)}$ operators:

$$[a^{(j_m)} \times \tilde{a}^{(j_{m'})}]^{(0)}. \quad (5)$$

These two operators of the second quantization are in a normal form, act on the same subshell m and represent the scalar operator for this first type (1) and (2) of valence–valence correlations. Therefore, this operator can be expressed through the operator of subshell occupation number \hat{N} on which it acts:

$$[a^{(j_m)} \times \tilde{a}^{(j_m)}]^{(0)} = -\frac{\hat{N}_m}{\sqrt{j_m}}. \quad (6)$$

There is no need to use the spin-angular program library `librang` [29] to calculate this diagram, as the spin-angular coefficient is expressed through a simple multiplier [30, A3]. This is one of the advantages of the methodology proposed in this paper.

VV_2 is a two-particle Feynman diagram, where its tensorial part is expressed through the tensorial product of creation $a^{(j)}$ and annihilation $\tilde{a}^{(j)}$ operators and represents the scalar operator (see Ref. [3], Section 2.3 and Fig. 2 there for more details):

$$[[a^{(j_m)} \times \tilde{a}^{(j_{m'})}]^{(j_{12})} \times [a^{(j_n)} \times \tilde{a}^{(j_{n'})}]^{(j_{12})}]^{(0)}. \quad (7)$$

For this VV_2 diagram, unlike for the VV_1 Feynman diagram considered above, there comes the additive summation, where the summation parameter j_{12} relates the tensor product (7) to the two $6j$ -coefficients. This summation parameter is the intermediate rank of this tensor product. All operators of the second quantization act on the same subshell m , therefore the tensorial operator (7) can be expressed through simple two \hat{N} operators in the case of $j_{12} = 0$:

$$[[a^{(j_m)} \times \tilde{a}^{(j_m)}]^{(0)} \times [a^{(j_m)} \times \tilde{a}^{(j_m)}]^{(0)}]^{(0)} = \frac{\hat{N}_m^2}{[j_m]}. \quad (8)$$

So for this case, for the calculation of the VV_2 diagram, we also do not need to use the spin-angular program library `librang` [29]. Meanwhile, the program library `librang` [29] from GRASP supports the calculation of the spin-angular part (7) of VV_2 Feynman diagram in the case of $j_{12} > 0$. Full Racah algebra [15–18] including the quasispin [22] is available for the integration of the spin-angular part of this Feynman diagram (see Ref. [29], Eqs. (29) and (30) therein). This is yet another advantage of the methodology proposed in this paper.

2.2. The second type of valence–valence correlations

This type of valence–valence correlations is presented through the Feynman diagram VV_2 from Fig. 2, where all lines with a double arrow of diagrams are renamed in the following way: $m' \equiv m$ and $n' \equiv n$:

$$\begin{aligned}
 & (n_m \ell_m) j_m^{w_m} (n_n \ell_n) j_n^{w_n} \rightarrow \\
 & \rightarrow (n_m \ell_m) j_m^{w_{m-1}} (n_n \ell_n) j_n^{w_{n-1}} (n_r \ell_r) j_r (n_s \ell_s) j_s,
 \end{aligned} \quad (9)$$

$$(n_m \ell_m) j_m^{w_m} (n_n \ell_n) j_n^{w_n} \rightarrow \\ \rightarrow (n_m \ell_m) j_m^{w_m-1} (n_n \ell_n) j_n^{w_n-1} (n_s \ell_s) j_s^2. \quad (10)$$

In this case, the tensorial part of the VV_2 diagram has the form

$$[[a^{(j_m)} \times \tilde{a}^{(j_m)}]^{(j_{12})} \times [a^{(j_n)} \times \tilde{a}^{(j_n)}]^{(j_{12})}]^{(0)}, \quad (11)$$

which can be expressed in the case of $j_{12} = 0$ as

$$[[a^{(j_m)} \times \tilde{a}^{(j_m)}]^{(0)} \times [a^{(j_n)} \times \tilde{a}^{(j_n)}]^{(0)}]^{(0)} = \\ = \frac{\hat{N}_m \hat{N}_n}{\sqrt{[j_m, j_n]}}. \quad (12)$$

So for this case, we also do not need to use the spin-angular program library `librang` [29] for the calculation of the VV_2 diagram. Meanwhile, the program library `librang` [29] from GRASP supports the calculation of the spin-angular part (11) of VV_2 Feynman diagram in the case of $j_{12} > 0$. Full Racah algebra [15–18] including the quasispin [22] is available for the integration of the spin-angular part of this Feynman diagram (see Ref. [29], Eqs. (26), (12) and (13) therein).

2.3. The contribution of valence–valence correlations to off-diagonal matrix elements

The main contribution of valence–valence correlations to off-diagonal matrix elements is in the matrix element $\langle (n_m \ell_m) j_m^{w_m} (n_n \ell_n) j_n^{w_n} || \hat{\mathcal{H}}_{\text{Effective}}^{(2)} || (n_m \ell_m) j_m^{w_m-2} (n_n \ell_n) j_n^{w_n+2} \rangle$. The above contribution is derived from the excitation

$$(n_m \ell_m) j_m^{w_m} (n_n \ell_n) j_n^{w_n} \rightarrow \\ \rightarrow (n_m \ell_m) j_m^{w_m-2} (n_n \ell_n) j_n^{w_n} (n_r \ell_r) j_r (n_s \ell_s) j_s \quad (13)$$

and can be described through the same two-particle Feynman diagram from Fig. 2, as above. This type of valence–valence correlations is presented through the Feynman diagram VV_2 , where all lines with a double arrow of the diagram are renamed in the following way: $m' \equiv n$, $n \equiv m$ and $n' \equiv n$.

In this case, the tensorial part of the VV_2 diagram has the following form:

$$[[a^{(j_n)} \times \tilde{a}^{(j_m)}]^{(j_{12})} \times [a^{(j_n)} \times \tilde{a}^{(j_m)}]^{(j_{12})}]^{(0)}. \quad (14)$$

In this case, after some modifications similar to those made in Section 3 of Ref. [21], the Racah algebra [15–18, 22] and the software library `librang` [29] are also fully available (see Ref. [29], Eqs. (26), (12) and (13) therein).

2.4. The remaining type of valence–valence correlations

The remaining types of valence–valence correlations

$$(n_m \ell_m) j_m^{w_m} (n_n \ell_n) j_n^{w_n} \rightarrow \\ \rightarrow (n_m \ell_m) j_m^{w_m+1} (n_n \ell_n) j_n^{w_n-2} (n_r \ell_r) j_r, \quad (15)$$

$$(n_m \ell_m) j_m^{w_m} (n_n \ell_n) j_n^{w_n} (n_p \ell_p) j_p^{w_p} \rightarrow \\ \rightarrow (n_m \ell_m) j_m^{w_m+1} (n_n \ell_n) j_n^{w_n-1} (n_p \ell_p) j_p^{w_p-1} (n_r \ell_r) j_r \quad (16)$$

are impossible to be included via RSMBPT without the improvement of the spin-angular program library `librang` [29]. This is related to the fact that these types of correlations are described by a three-particle Feynman diagram. The index p in Eq. (16) belongs to the space F' , as do the indices n and m .

3. Combination of the RCI approximation with stationary second-order Rayleigh–Schrödinger many-body perturbation theory

Similar to CV, C and CC correlations [3–5], the admixed configurations from VV correlations (Eqs. (1), (2), (9) and (10)) can be added to the usual energy $E_0(K)$ of the term χJ of the configuration K and can be expressed as the energy $\Delta E_0(KJ)$, which does not depend on the term, and the sum of the product of Slater integrals and spin-angular coefficients, describing the interaction within open subshells and between them:

$$E(K \chi J) = \\ = E_0(KJ) + \Delta E_0(KJ) + \\ + \sum_{n \ell j} \sum_{k > 0} \tilde{f}_k(\ell j^w, K \chi J) \times \\ \times [\mathcal{F}^k(n \ell j, n \ell j) + \Delta \mathcal{F}^k(n \ell j, n \ell j)] + \\ + \sum_{n \ell j} \sum_{n' \ell' j' > n \ell j} \left\{ \sum_{k > 0} \tilde{f}_k(\ell j^w \ell' j'^w, K \chi J) \times \right. \\ \times [\mathcal{F}^k(n \ell j, n' \ell' j') + \Delta \mathcal{F}^k(n \ell j, n' \ell' j')] + \quad (17)$$

$$\begin{aligned}
& + \sum_k \tilde{g}_k(\ell j^w \ell' j'^{w'}, K \chi J) \times \\
& \times [\mathcal{G}^k(nlj, n'\ell'j') + \Delta \mathcal{G}^k(nlj, n'\ell'j')] + \\
& + \sum_k \tilde{v}_k(\ell j^w \ell' j'^{w'}, \ell j^{w-2} \ell' j'^{w+2}, K \chi J K' \chi' J) \times \\
& \times [\mathcal{R}^k(nlj, n'\ell'j'n'\ell'j') + \\
& + \Delta \mathcal{R}^k(nlj, n'\ell'j'n'\ell'j')], \quad (17 \text{ continued})
\end{aligned}$$

Here \tilde{f}_k , \tilde{g}_k and \tilde{v}_k are spin-angular coefficients from which submatrix elements $\langle \ell j || C^{(k)} || \ell' j' \rangle$ are extracted. Therefore, the summation over k runs over all possible values instead of the values which satisfy the triangular condition $(\ell \ell' k)$ as it is in the ordinary case. $\mathcal{F}^k(nlj, n'\ell'j')$, $\mathcal{G}^k(nlj, n'\ell'j')$ and $\mathcal{R}^k(nlj, n'\ell'j'n'\ell'j')$ are the generalized integrals of the electrostatic interaction between electrons. The definition of $\mathcal{R}^k(nlj, n'\ell'j'n'\ell'j')$ is

$$\begin{aligned}
& \mathcal{R}^k(ij, i'j') \\
& = \{[1 + \delta(i, j)] [1 + \delta(i', j')]\}^{-1/2} R^k(n_i j_i n_j j_j, n_{i'} j_{i'} n_{j'} j_{j'}) \\
& \times \langle \ell_i j_i || C^{(k)} || \ell_{i'} j_{i'} \rangle \langle \ell_{j'} j_j || C^{(k)} || \ell_{j'} j_j \rangle, \quad (18)
\end{aligned}$$

where $R^k(n_i j_i n_j j_j, n_{i'} j_{i'} n_{j'} j_{j'})$ is the same radial integral as in Eq. (4). Definitions of $\mathcal{F}^k(nlj, n'\ell'j')$ and $\mathcal{G}^k(nlj, n'\ell'j')$ straightforwardly follow from Eq. (18).

The contribution coming from the VV correlations of the configurations K' to $E(K \chi J)$ in the second order of the perturbation theory can be written from Eq. (17) as

$$\begin{aligned}
& \Delta E_{\text{PT(VV)}} = \Delta \mathcal{E}_0(KJ) + \\
& + \sum_{nlj} \sum_{k>0} \tilde{f}_k(\ell j^w, K \chi J) \times \\
& \times \Delta \mathcal{F}^k(nlj, nlj) + \\
& + \sum_{nlj} \sum_{n'\ell'j'>nlj} \left\{ \sum_{k>0} \tilde{f}_k(\ell j^w \ell' j'^{w'}, K \chi J) \times \right. \\
& \times \Delta \mathcal{F}^k(nlj, n'\ell'j') + \\
& + \sum_k \tilde{g}_k(\ell j^w \ell' j'^{w'}, K \chi J) \Delta \mathcal{G}^k(nlj, n'\ell'j') + \\
& + \sum_k \tilde{v}_k(\ell j^w \ell' j'^{w'}, \ell j^{w-2} \ell' j'^{w+2}, K \chi J K' \chi' J) \times \\
& \times \left. \Delta \mathcal{R}^k(nlj, n'\ell'j'n'\ell'j') \right\}. \quad (19)
\end{aligned}$$

The contribution of the first and second type of the VV correlations in the second order of

the perturbation theory is expressed over $\Delta \mathcal{E}_0(KJ)$, $\Delta \mathcal{F}^k(nlj, nlj)$, $\Delta \mathcal{F}^k(nlj, n'\ell'j')$ and $\Delta \mathcal{G}^k(nlj, n'\ell'j')$ (see Tables 1 and 2). These formulae are additionally expressed via the quantities

$$\begin{aligned}
& \mathcal{A}'(x, ij, i'j') = \\
& = \sum_{k,k'} \left\{ \begin{array}{c} k \ k' \ x \\ j_i \ j_i \ j_{i'} \end{array} \right\} \left\{ \begin{array}{c} k \ k' \ x \\ j_j \ j_j \ j_{j'} \end{array} \right\} \mathcal{P}(kk', ij, i'j'), \quad (20)
\end{aligned}$$

and

$$\begin{aligned}
& \mathcal{B}(x, ij, i'j') = \\
& = \sum_{k,k'} \left\{ \begin{array}{c} k \ k' \ x \\ j_j \ j_i \ j_{i'} \end{array} \right\} \left\{ \begin{array}{c} k \ k' \ x \\ j_i \ j_j \ j_{j'} \end{array} \right\} Q(kk', ij, i'j'), \quad \text{where} \quad (21)
\end{aligned}$$

$$\mathcal{P}(kk', ij, i'j') = \mathcal{R}^k(ij, i'j') \mathcal{R}^k(i'j', ij) \mathcal{O}(K', K), \quad (22)$$

$$Q(kk', ij, i'j') = \mathcal{R}^k(ij, i'j') \mathcal{R}^k(i'j', ji) \mathcal{O}(K', K), \quad (23)$$

$$\mathcal{O}(K', K) = \frac{1}{\bar{E}(K') - \bar{E}(K)}, \quad (24)$$

where $\bar{E}(K)$ is the averaged energy of the state for which calculations are performed. $\bar{E}(K')$ is the averaged energy for the admixed configuration K' . For details on how to find $\bar{E}(K)$ and $\bar{E}(K')$, see Ref. [3], Section 3. We would like to emphasize that the energy denominator (24) is defined differently/opposite to the expressions of Feynman diagrams (see, for example, Fig. 1, Eqs. (22, 23)).

As we can see, the expression of the first type of valence–valence correlations for the contribution $\Delta \mathcal{E}_0$ (see Table 1) depends on the occupation number w_m of the subshell m (number of electrons in the subshell m). This is due to the fact that the first type of valence–valence correlations is described by the VV₁ and VV₂ Feynman diagrams, the angular part of which is expressed via the operator \hat{N} of the subshell occupation number (see Eqs. (6) and (8)). Meanwhile, the second type of valence–valence correlations for the contribution $\Delta \mathcal{E}_0$ described only by the VV₂ Feynman diagram depends on the occupation number w_m of the subshell m and on the occupation number w_n of the subshell n because the tensorial part of the diagram (see Eq. (12)) acts on these two subshells separately.

The contribution of VV correlation in the second order of perturbation theory coming from the off-diagonal matrix element $\langle (n_m \ell_m) j_m^{w_m} (n_n \ell_n) j_n^{w_n} | \hat{\mathcal{H}}_{\text{Effective}}^{(2)} | (n_m \ell_m) j_m^{w_m-2} (n_n \ell_n) j_n^{w_n+2} \rangle$ is described by the diagram VV₂. Reformulation of the expressions of this diagram into the form suitable for the GRASP

Table 1. Expressions for both two types (where $s \neq r$ or $s = r$) of valence–valence corrections to the energy in Eq. (17), independent of the term.

$\Delta\epsilon_0$ corrections
$(n_m \ell_m) j_m^{w_m} (n_n \ell_n) j_n^{w_n} \rightarrow (n_m \ell_m) j_m^{w_m-2} (n_n \ell_n) j_n^{w_n} (n_r \ell_r) j_r (n_s \ell_s) j_s$ $-\frac{2w_m(w_m-1)}{[j_m]} \mathcal{A}'(0, mm, rs)$ <p style="text-align: center;">from VV_1 and VV_2 Feynman diagrams</p>
$(n_m \ell_m) j_m^{w_m} (n_n \ell_n) j_n^{w_n} \rightarrow (n_m \ell_m) j_m^{w_m-1} (n_n \ell_n) j_n^{w_n-1} (n_r \ell_r) j_r (n_s \ell_s) j_s$ $-\frac{w_m w_n}{\sqrt{[j_m, j_n]}} [\mathcal{A}'(0, mn, rs) + \mathcal{A}'(0, mn, sr)]$ <p style="text-align: center;">from VV_2 Feynman diagram</p>

Table 2. Expressions for Slater integrals $\Delta\mathcal{F}^k(m, m)$, $\Delta\mathcal{F}^k(m, n)$ and $\Delta\mathcal{G}^k(m, n)$ (see Eq. (17)) corresponding to both two types (where $s \neq r$ or $s = r$) of valence–valence corrections.

Corrections	Slater integral	k values
$(n_m \ell_m) j_m^{w_m} (n_n \ell_n) j_n^{w_n} \rightarrow (n_m \ell_m) j_m^{w_m-2} (n_n \ell_n) j_n^{w_n} (n_r \ell_r) j_r (n_s \ell_s) j_s$ $\underbrace{-4[k]\mathcal{A}'(k, mm, rs)}_{\text{from } VV_1 \text{ and } VV_2 \text{ Feynman diagrams}}$	$\Delta\mathcal{F}^k(m, m)$	$k > 0$
$(n_m \ell_m) j_m^{w_m} (n_n \ell_n) j_n^{w_n} \rightarrow (n_m \ell_m) j_m^{w_m-1} (n_n \ell_n) j_n^{w_n-1} (n_r \ell_r) j_r (n_s \ell_s) j_s$ $\underbrace{-[k](\mathcal{A}'(k, mn, rs) + \mathcal{A}'(k, mn, sr))}_{\text{from } VV_2 \text{ Feynman diagram}}$	$\Delta\mathcal{F}^k(m, n)$	$k > 0$
$\underbrace{-2[k]\mathcal{B}(k, mn, rs)}_{\text{from } VV_2 \text{ Feynman diagram}}$	$\Delta\mathcal{G}^k(m, n)$	$k \geq 0$

Table 3. Expressions for Slater integrals $\Delta\mathcal{R}^k(mm, nn)$ (see Eq. (17)) corresponding to the valence–valence $(n_m \ell_m) j_m^{w_m} (n_n \ell_n) j_n^{w_n} \rightarrow (n_m \ell_m) j_m^{w_m-2} (n_n \ell_n) j_n^{w_n} (n_r \ell_r) j_r (n_s \ell_s) j_s$ corrections coming from the off-diagonal matrix element $\langle (n_m \ell_m) j_m^{w_m} (n_n \ell_n) j_n^{w_n} | \mathcal{H}_{\text{Effective}}^{(2)} | (n_m \ell_m) j_m^{w_m-2} (n_n \ell_n) j_n^{w_n+2} \rangle$.

Corrections	Slater integral	k values
$\underbrace{-4[k]\chi(k, mm, rs, nn)}_{\text{from } VV_2 \text{ Feynman diagram}}$	$\Delta\mathcal{R}^k(mm, nn)$	$k \geq 0$

gave these corrections only to the radial integral $\Delta\mathcal{R}^k(mm, nn)$ (see Table 3). This formula is expressed via the quantity

$$\begin{aligned} \chi(x, ij, i'j', i''j'') &= \\ &= \sum_{k,k'} \left\{ \begin{matrix} k & k' & x \\ j_{i''} & j_i & j_{i'} \end{matrix} \right\} \left\{ \begin{matrix} k & k' & x \\ j_{j''} & j_j & j_{j'} \end{matrix} \right\} \mathcal{S}'(kk', ij, i'j', i''j''), \end{aligned} \quad (25)$$

where

$$\begin{aligned} \mathcal{S}'(kk', ij, i'j', i''j'') &= \\ &= \mathcal{R}^k(ij, i'j') \mathcal{R}^k(i'j', i''j'') \mathcal{O}(K', K_1 K_2) \end{aligned} \quad (26)$$

and

$$\begin{aligned} \mathcal{O}(K', K_1 K_2) &= \\ &= \frac{1}{2} \left(\frac{1}{E(K') - E(K_1)} + \frac{1}{E(K') - E(K_2)} \right), \end{aligned} \quad (27)$$

where $\bar{E}(K_1)$ corresponds to the averaged energy of the configuration K_1 from the bra function of the off-diagonal matrix element and $\bar{E}(K_2)$ corresponds to the averaged energy of the configuration K_1 from the ket function of the off-diagonal matrix element. For details on how to find them, see Ref. [3], Section 3.

This theory in an irreducible tensorial form is more suitable to be included in such a version of the GRASP which is based on configuration state function generators [31]. This is related to the fact that this version of the software package allows us to distinguish F , F' and G sets of orbitals very easily in the process of computing atomic data. In the following Section, we will present a test case of this implementation.

4. Calculation of core-valence, core, core–core and valence–valence correlations with a new approach

In the present work, the method based on Rayleigh–Schrödinger perturbation theory in an irreducible tensorial form [3–5] is extended to include VV correlations in the computations. Firstly, we present the results when only VV correlations are included in a regular way and using the stationary second-order Rayleigh–Schrödinger many-body perturbation theory in an irreducible tensorial form. For this purpose, we computed the 105 lowest energy levels of the $4s^24p^2$, $4p^4$, $4s^24p\{4d, 4f, 5s, 5p, 5d, 6s, 6p\}$, $4s4p^3$ and $4s4p^2\{4d, 5s\}$ configurations of Se III. Furthermore, we performed calculations using the regular way and the RSMBPT method when CV, C, CC and VV correlations are included. To reduce the computational resources, these calculations are performed for the Se III energy levels of the even configurations with $J = 0$ and the levels of the odd configurations with $J = 1$. The radial wave functions for all abovementioned computations are taken from the earlier study [32]. The multireference (MR) set in the present calculations consists of the $4s^24p^2$, $4p^4$, $4s^24p\{4f, 5p, 6p\}$, $4s4p^2\{4d, 5s\}$ even and $4s^24p\{4d, 5s, 5d, 6s\}$, $4s4p^3$ odd configurations. It should be noted that the MR set in the present computations consists of orbitals with few different principal quantum numbers, namely with n , $n + 1$ and $n + 2$ (where $n = 4$). Such calculations are carried out using both the regular RCI and the RCI (RSMBPT) methods. The RCI

calculations are performed, including the Coulomb and Breit interactions and leading quantum electrodynamic effects – vacuum polarization and self-energy corrections. Meanwhile, the estimation of correlations was done using the stationary second-order Rayleigh–Schrödinger many-body perturbation theory in an irreducible tensorial form for the Coulomb interaction. The calculations using both the regular RCI and RCI (RSMBPT) methods were performed including only CSFs that have non-zero matrix elements in the sets of spin-angular integration with the CSFs belonging to the configurations in the MR set.

4.1. Computational schemes

Regular RCI computations including VV correlations are marked as **VV RCI**. In this computational scheme, single–double (SD) substitutions are allowed from the $4s$, $4p$, $4p$, $4d$, $4d$, $4f$, $4f$, $5s$, $5p$, $5p$, $5d$, $5d$, $6s$, $6p$, $6p$ valence orbitals of the MR set to the orbital set (OS) $OS_1 = \{7s, 7p, 7p, 6d, 6d, 5f, 5f, 5g, 5g\}, \dots, OS_4 = \{10s, 10p, 10p, 9d, 9d, 8f, 8f, 8g, 8g\}$. In the **CV+C+CC+VV RCI** computational scheme, SD substitutions are allowed from the valence orbitals (mentioned above) and from the $3s$, $3p$, $3p$, $3d$ and $3d$ core orbitals to the orbital set OS_1, \dots, OS_4 .

The CSF space in the computations using the RSMBPT method is divided into three sets: F , F' and G (see Ref. [3] for details). The $1s$, $2s$, $2p$, $2p$, $3s$, $3p$, $3p$, $3d$ and $3d$ subshells are defined as core subshells (that correspond to the F set), $4s$, $4p$, $4p$, $4d$, $4d$, $4f$, $5s$, $5p$, $5p$, $5d$, $5d$, $6s$, $6p$, $6p$ as valence subshells (that correspond to the F' set) and the subshells belonging to OS_1, \dots, OS_4 as virtual ones (that correspond to the G set). In the calculations when only VV correlations are included, all core subshells are inactive, in the case including CV, C, CC and VV correlations, the $1s$, $2s$, $2p$ and $2p$ subshells are defined as inactive core subshells, and $3s$, $3p$, $3p$, $3d$ and $3d$ subshells are defined as active core subshells. This space distribution is consistent with regular GRASP2018 calculations and allows the use of a combination of RCI and RSMBPT methods.

The RSMBPT calculation procedure is analogous to that used in the previous research [3–5]. The contribution of each K' configuration to CSF for which energy needs to be calculated according

to Rayleigh–Schrödinger perturbation theory in an irreducible tensorial form is computed according to Eq. (22) of Ref. [3] (for CV correlations), Eq. (6) of Ref. [4] (for C correlations), Eq. (26) of Ref. [5] (for CC correlations) and Eq. (19) (for VV correlations). K' configurations are sorted in a descending order according to the impact of the correlations for each level. Further, K' configurations are selected by the impact of VV (for calculations when only VV correlations included) or CV, C, CC and VV (for calculations when all correlations are included) correlations with the specified fraction (expressed in the percentage: 95, 99, 99.5, 99.95 and 100%) of the total correlations contribution, and RCI computations are performed including them. It should be noted that the program gives the contribution of the correlations of K' configuration with a value greater than 1.0E–11. Contributions of smaller magnitudes are neglected. The C correlations (Eq. (3) of Ref. [4]), CV correlations (Eq. (4) of Ref. [4]) and VV correlations (Eqs. (15) and (16)), which are not included in the RSMBPT method, were added to the RCI calculations in a regular way. The results that include VV correlations according to the RSMBPT method are marked as **VV RCI (RSMBPT)**. The results including CV, C, CC and VV correlations according to the RSMBPT method are marked as **CV+C+CC+VV RCI (RSMBPT)**.

4.2. Results

4.2.1. Valence–valence correlations

Table 4 presents a comparison of the total energies from the regular RCI (**VV RCI**) and from the RSMBPT (**VV RCI (RSMBPT)**) calculations for 105 energy levels of the Se III. In the Table, the total energies from the **VV RCI** calculations and the energy differences between the **VV RCI (RSMBPT)** and **VV RCI** calculations are given. The last line of the Table gives the number of CSFs (N_{CSFs}) for each computational scheme. As seen from the Table, including the most significant VV correlations by increasing the amount of these correlations (95, 99, 99.5, 99.95 and 100%), the results converge to the regular GRASP2018 results, and in the case of ‘100%’ reproduce them. In the case of ‘100%’ for the majority of levels, the agreement is excellent, this discrepancy between **VV RCI (RSMBPT)** and **VV RCI** is very small and reaches only up to 4.9E–05 a.u. (or 0.000002%).

Table 5 compares the energy levels from the regular RCI and RSMBPT computations when only VV correlations are included. It is seen from this Table that by adding the most important K' configurations of VV correlations step by step, the **VV RCI (RSMBPT)** results converge to the results of regular GRASP2018 calculations. The largest

Table 4. The total energies (in a.u.) from the **VV RCI** calculations and differences (in a.u.) between the **VV RCI (RSMBPT)** and **VV RCI** energies ($\Delta E_{(\text{VV RCI (RSMBPT)})-(\text{VV RCI})}$) for Se III are given when the VV correlations are included in the computations.

No.	State	VV RCI	$\Delta E_{(\text{VV RCI (RSMBPT)})-(\text{VV RCI})}$				
			95%	99%	99.5%	99.95%	100%
1	$4s^24p^2\ ^3P_0$	–2425.6827502	0.0001895	0.0000309	0.0000202	0.0000120	0.0000027
2	$4s^24p^2\ ^3P_1$	–2425.6753106	0.0001577	0.0000308	0.0000165	0.0000038	0.0000020
3	$4s^24p^2\ ^3P_2$	–2425.6656787	0.0001364	0.0000256	0.0000117	0.0000025	0.0000021
4	$4s^24p^2\ ^1D_2$	–2425.6233754	0.0002463	0.0000542	0.0000263	0.0000042	0.0000031
5	$4s^24p^2\ ^1S_0$	–2425.5540801	0.0002955	0.0000689	0.0000330	0.0000252	0.0000014
6	$4s4p^3\ ^5S_2^o$	–2425.3865441	0.0000772	0.0000170	0.0000081	0.0000010	0.0000000
7	$4s4p^3\ ^3D_1^o$	–2425.2728556	0.0001927	0.0000496	0.0000340	0.0000121	0.0000071
8	$4s4p^3\ ^3D_2^o$	–2425.2722502	0.0001830	0.0000383	0.0000222	0.0000084	0.0000072
9	$4s4p^3\ ^3D_3^o$	–2425.2696375	0.0001987	0.0000466	0.0000291	0.0000100	0.0000058
10	$4s4p^3\ ^3P_2^o$	–2425.2080103	0.0002059	0.0000384	0.0000211	0.0000044	0.0000027
11	$4s4p^3\ ^3P_0^o$	–2425.2077293	0.0002487	0.0000750	0.0000402	0.0000122	0.0000010
12	$4s4p^3\ ^3P_1^o$	–2425.2077069	0.0003106	0.0000564	0.0000395	0.0000102	0.0000041

Table 4. (continued)

No.	State	VV RCI	$\Delta E_{(\text{VV RCI (RSMBPT)})-(\text{VV RCI})}$				
			95%	99%	99.5%	99.95%	100%
13	$4s^24p4d\ ^1D_2^o$	-2425.1795605	0.0001731	0.0000333	0.0000215	0.0000076	0.0000062
14	$4s^24p4d\ ^3F_2^o$	-2425.1264631	0.0002440	0.0000663	0.0000457	0.0000271	0.0000239
15	$4s^24p4d\ ^3F_3^o$	-2425.1204839	0.0002133	0.0000474	0.0000303	0.0000125	0.0000092
16	$4s^24p5s\ ^3P_0^o$	-2425.1130178	0.0002397	0.0000860	0.0000682	0.0000445	0.0000342
17	$4s^24p5s\ ^3P_1^o$	-2425.1107765	0.0001492	0.0000293	0.0000167	0.0000036	0.0000020
18	$4s^24p4d\ ^3F_4^o$	-2425.1102801	0.0003001	0.0000771	0.0000460	0.0000069	0.0000002
19	$4s^24p5s\ ^3P_2^o$	-2425.0952711	0.0001736	0.0000404	0.0000244	0.0000038	0.0000006
20	$4s^24p5s\ ^1P_1^o$	-2425.0877335	0.0001506	0.0000248	0.0000145	0.0000022	0.0000010
21	$4s^24p4d\ ^1P_1^o$	-2425.0559576	0.0002530	0.0000591	0.0000391	0.0000191	0.0000164
22	$4s^24p4d\ ^3P_2^o$	-2425.0487287	0.0003104	0.0000608	0.0000333	0.0000077	0.0000044
23	$4s^24p4d\ ^3D_1^o$	-2425.0469453	0.0002286	0.0000543	0.0000329	0.0000141	0.0000097
24	$4s^24p4d\ ^3P_1^o$	-2425.0367313	0.0002198	0.0000538	0.0000344	0.0000169	0.0000150
25	$4s^24p4d\ ^3D_3^o$	-2425.0365571	0.0002450	0.0000468	0.0000313	0.0000119	0.0000086
26	$4s^24p4d\ ^3P_0^o$	-2425.0361679	0.0003669	0.0001383	0.0001016	0.0000676	0.0000490
27	$4s^24p4d\ ^3D_2^o$	-2425.0342497	0.0002600	0.0000569	0.0000399	0.0000179	0.0000155
28	$4s4p^3\ ^3S_1^o$	-2425.0324298	0.0002367	0.0000602	0.0000432	0.0000116	0.0000077
29	$4s^24p4d\ ^1F_3^o$	-2425.0072526	0.0003419	0.0000807	0.0000468	0.0000253	0.0000191
30	$4s^24p5p\ ^1P_1$	-2425.0038073	0.0001521	0.0000368	0.0000242	0.0000108	0.0000006
31	$4s4p^3\ ^1D_2^o$	-2425.0023171	0.0002710	0.0000591	0.0000397	0.0000162	0.0000143
32	$4s^24p5p\ ^3D_1$	-2424.9927206	0.0001462	0.0000408	0.0000220	0.0000082	0.0000005
33	$4s^24p5p\ ^3D_2$	-2424.9911607	0.0001331	0.0000320	0.0000181	0.0000038	0.0000006
34	$4s^24p5p\ ^3P_0$	-2424.9849192	0.0001334	0.0000262	0.0000187	0.0000081	0.0000006
35	$4s^24p5p\ ^3P_1$	-2424.9785409	0.0001262	0.0000312	0.0000184	0.0000065	0.0000003
36	$4s^24p5p\ ^3D_3$	-2424.9774657	0.0002120	0.0000616	0.0000335	0.0000115	0.0000001
37	$4s^24p5p\ ^3P_2$	-2424.9716950	0.0001131	0.0000241	0.0000139	0.0000033	0.0000005
38	$4s^24p5p\ ^3S_1$	-2424.9652235	0.0001870	0.0000613	0.0000375	0.0000163	0.0000001
39	$4s4p^3\ ^1P_1^o$	-2424.9597596	0.0003101	0.0000696	0.0000445	0.0000153	0.0000113
40	$4s^24p5p\ ^1D_2$	-2424.9561445	0.0001302	0.0000278	0.0000162	0.0000037	0.0000011
41	$4s^24p5p\ ^1S_0$	-2424.9308286	0.0001819	0.0000432	0.0000246	0.0000088	0.0000005
42	$4s^24p6s\ ^3P_0^o$	-2424.8379021	0.0001859	0.0000590	0.0000462	0.0000302	0.0000232
43	$4s^24p6s\ ^3P_1^o$	-2424.8368552	0.0001271	0.0000222	0.0000120	0.0000035	0.0000028
44	$4s^24p5d\ ^3F_2^o$	-2424.8330064	0.0001443	0.0000349	0.0000248	0.0000091	0.0000067
45	$4s^24p5d\ ^3F_3^o$	-2424.8272709	0.0001368	0.0000272	0.0000143	0.0000040	0.0000018
46	$4s^24p4f\ ^1F_3$	-2424.8271943	0.0001997	0.0000591	0.0000337	0.0000124	0.0000065
47	$4s^24p4f\ ^3F_3$	-2424.8257288	0.0001971	0.0000364	0.0000256	0.0000068	0.0000016
48	$4s^24p4f\ ^3F_2$	-2424.8249661	0.0001671	0.0000318	0.0000242	0.0000101	0.0000091
49	$4s^24p5d\ ^3D_2$	-2424.8245284	0.0001321	0.0000208	0.0000124	0.0000027	0.0000015
50	$4s^24p4f\ ^3F_4$	-2424.8245239	0.0001761	0.0000459	0.0000235	0.0000042	0.0000003
51	$4s^24p5d\ ^3D_1^o$	-2424.8207738	0.0001337	0.0000216	0.0000144	0.0000070	0.0000056
52	$4s^24p6s\ ^3P_2^o$	-2424.8187223	0.0001537	0.0000313	0.0000205	0.0000038	0.0000012

Table 4. (continued)

No.	State	VV RCI	$\Delta E_{(VV\ RCI\ (RSMBPT))-(VV\ RCI)}$				
			95%	99%	99.5%	99.95%	100%
53	$4s4p^2\ ^4P\ 4d\ ^3P_2$	-2424.8178397	0.0001080	0.0000235	0.0000111	0.0000047	0.0000036
54	$4s^24p6s\ ^1P_1^o$	-2424.8156645	0.0001222	0.0000183	0.0000103	0.0000027	0.0000018
55	$4s^24p5d\ ^3F_4^o$	-2424.8138892	0.0001600	0.0000341	0.0000198	0.0000033	0.0000001
56	$4s4p^2\ ^4P\ 4d\ ^5F_1$	-2424.8119309	0.0001347	0.0000325	0.0000212	0.0000086	0.0000051
57	$4s^24p4f\ ^3G_3$	-2424.8105949	0.0001999	0.0000552	0.0000368	0.0000159	0.0000097
58	$4s^24p5d\ ^1D_2^o$	-2424.8103478	0.0001300	0.0000246	0.0000162	0.0000064	0.0000050
59	$4s4p^2\ ^4P\ 4d\ ^5F_2$	-2424.8097339	0.0001026	0.0000232	0.0000138	0.0000050	0.0000043
60	$4s^24p4f\ ^3G_4$	-2424.8091362	0.0001252	0.0000385	0.0000273	0.0000053	0.0000010
61	$4s4p^2\ ^4P\ 4d\ ^3P_1$	-2424.8091238	0.0001718	0.0000372	0.0000161	0.0000050	0.0000025
62	$4s^24p5d\ ^3D_3^o$	-2424.8072808	0.0001359	0.0000257	0.0000171	0.0000053	0.0000035
63	$4s4p^2\ ^4P\ 4d\ ^5F_3$	-2424.8063898	0.0001154	0.0000269	0.0000180	0.0000079	0.0000031
64	$4s4p^2\ ^4P\ 4d\ ^3P_0$	-2424.8060102	0.0001349	0.0000239	0.0000152	0.0000052	0.0000009
65	$4s^24p4f\ ^3G_5$	-2424.8058236	0.0002456	0.0000808	0.0000445	0.0000118	0.0000003
66	$4s^24p5d\ ^3P_2^o$	-2424.8038729	0.0001341	0.0000273	0.0000168	0.0000060	0.0000045
67	$4s^24p4f\ ^3D_3$	-2424.8033484	0.0001971	0.0000414	0.0000256	0.0000070	0.0000009
68	$4s^24p5d\ ^3P_1^o$	-2424.8029622	0.0001490	0.0000402	0.0000253	0.0000096	0.0000074
69	$4s^24p4f\ ^3D_2$	-2424.8021879	0.0001782	0.0000370	0.0000246	0.0000089	0.0000070
70	$4s^24p5d\ ^3P_0^o$	-2424.8020585	0.0001877	0.0000501	0.0000346	0.0000204	0.0000130
71	$4s4p^2\ ^4P\ 4d\ ^5F_4$	-2424.8016324	0.0001099	0.0000219	0.0000143	0.0000041	0.0000016
72	$4s^24p4f\ ^1G_4$	-2424.7995880	0.0002058	0.0000625	0.0000403	0.0000074	0.0000022
73	$4s^24p4f\ ^3D_1$	-2424.7985206	0.0002064	0.0000403	0.0000283	0.0000085	0.0000044
74	$4s^24p4f\ ^1D_2$	-2424.7969189	0.0001596	0.0000366	0.0000215	0.0000024	0.0000007
75	$4s4p^2\ ^4P\ 4d\ ^5F_5$	-2424.7951151	0.0001537	0.0000455	0.0000311	0.0000127	0.0000005
76	$4s^24p5d\ ^1F_3^o$	-2424.7928576	0.0002132	0.0000466	0.0000275	0.0000127	0.0000085
77	$4s^24p6p\ ^3D_1$	-2424.7927791	0.0001832	0.0000451	0.0000280	0.0000100	0.0000013
78	$4s^24p6p\ ^3P_1$	-2424.7892989	0.0001538	0.0000366	0.0000209	0.0000054	0.0000006
79	$4s^24p6p\ ^3D_2$	-2424.7880545	0.0001348	0.0000276	0.0000164	0.0000021	0.0000006
80	$4s^24p5d\ ^1P_1^o$	-2424.7876585	0.0001892	0.0000410	0.0000291	0.0000106	0.0000076
81	$4s^24p6p\ ^3P_0$	-2424.7874870	0.0001368	0.0000279	0.0000208	0.0000065	0.0000005
82	$4s4p^2\ ^4P\ 4d\ ^5D_0$	-2424.7825283	0.0001321	0.0000315	0.0000210	0.0000072	0.0000034
83	$4s4p^2\ ^4P\ 4d\ ^5D_1$	-2424.7823026	0.0001235	0.0000296	0.0000195	0.0000072	0.0000036
84	$4s4p^2\ ^4P\ 4d\ ^5D_2$	-2424.7815098	0.0001067	0.0000222	0.0000145	0.0000044	0.0000033
85	$4s4p^2\ ^4P\ 4d\ ^5D_3$	-2424.7799579	0.0001435	0.0000322	0.0000226	0.0000093	0.0000024
86	$4s4p^2\ ^4P\ 4d\ ^5D_4$	-2424.7770902	0.0001382	0.0000297	0.0000208	0.0000064	0.0000013
87	$4s^24p6p\ ^1P_1$	-2424.7754567	0.0001410	0.0000353	0.0000209	0.0000055	0.0000008
88	$4s4p^2\ ^4P\ 5s\ ^5P_1$	-2424.7740592	0.0001216	0.0000344	0.0000226	0.0000044	0.0000010
89	$4s^24p6p\ ^3P_2$	-2424.7729862	0.0001384	0.0000327	0.0000169	0.0000033	0.0000012
90	$4s^24p6p\ ^3D_3$	-2424.7719517	0.0001989	0.0000506	0.0000271	0.0000077	0.0000003
91	$4p^4\ ^1D_2$	-2424.7709312	0.0001722	0.0000698	0.0000383	0.0000056	0.0000031
92	$4s^24p6p\ ^3S_1$	-2424.7681892	0.0001537	0.0000385	0.0000240	0.0000091	0.0000002
93	$4s4p^2\ ^4P\ 5s\ ^5P_2$	-2424.7675863	0.0000780	0.0000215	0.0000159	0.0000018	0.0000011

Table 4. (continued)

No.	State	VV RCI	$\Delta E_{(\text{VV RCI (RSMBPT)})-(\text{VV RCI})}$				
			95%	99%	99.5%	99.95%	100%
94	$4s^24p6p\ ^1D_2$	-2424.7652980	0.0001359	0.0000298	0.0000163	0.0000027	0.0000009
95	$4s4p^2\ ^4P\ 5s\ ^5P_3$	-2424.7593175	0.0000961	0.0000229	0.0000161	0.0000048	0.0000008
96	$4s^24p6p\ ^1S_0$	-2424.7562436	0.0001812	0.0000421	0.0000291	0.0000086	0.0000007
97	$4s4p^2\ ^4P\ 4d\ ^3F_2$	-2424.7533416	0.0002147	0.0001140	0.0000915	0.0000102	0.0000055
98	$4s4p^2\ ^4P\ 4d\ ^3F_3$	-2424.7483267	0.0002850	0.0001041	0.0000916	0.0000312	0.0000047
99	$4s4p^2\ ^4P\ 4d\ ^3F_4$	-2424.7411003	0.0002728	0.0000810	0.0000493	0.0000112	0.0000036
100	$4s4p^2\ ^4P\ 5s\ ^3P_0$	-2424.7382269	0.0002030	0.0000621	0.0000522	0.0000166	0.0000026
101	$4s4p^2\ ^4P\ 5s\ ^3P_1$	-2424.7330497	0.0002147	0.0000900	0.0000591	0.0000072	0.0000014
102	$4s4p^2\ ^4P\ 4d\ ^5P_3$	-2424.7304806	0.0001247	0.0000255	0.0000183	0.0000076	0.0000014
103	$4s4p^2\ ^4P\ 4d\ ^5P_2$	-2424.7277161	0.0000887	0.0000204	0.0000140	0.0000049	0.0000037
104	$4s4p^2\ ^4P\ 4d\ ^5P_1$	-2424.7255078	0.0001077	0.0000287	0.0000208	0.0000104	0.0000052
105	$4s4p^2\ ^4P\ 5s\ ^3P_2$	-2424.7232999	0.0001736	0.0000560	0.0000297	0.0000030	0.0000020
N_{CSFs}		285503	176181	219451	232906	259552	274526

Table 5. The energy levels (in cm^{-1}) and differences (in cm^{-1}) between the VV RCI (RSMBPT) and VV RCI energies ($\Delta E_{(\text{VV RCI (RSMBPT)})-(\text{VV RCI})}$) for Se III are given when the VV correlations are included in the computations.

No.	State	VV RCI	$\Delta E_{(\text{VV RCI (RSMBPT)})-(\text{VV RCI})}$				
			95%	99%	99.5%	99.95%	100%
1	$4s^24p^2\ ^3P_0$	0.00	0.00	0.00	0.00	0.00	0.00
2	$4s^24p^2\ ^3P_1$	1632.80	-6.98	-0.01	-0.81	-1.82	-0.15
3	$4s^24p^2\ ^3P_2$	3746.75	-11.65	-1.15	-1.86	-2.08	-0.12
4	$4s^24p^2\ ^1D_2$	13031.27	12.45	5.10	1.34	-1.73	0.07
5	$4s^24p^2\ ^1S_0$	28239.83	23.24	8.34	2.81	2.87	-0.29
6	$4s4p^3\ ^5S_2^o$	65009.71	-24.64	-3.03	-2.62	-2.42	-0.59
7	$4s4p^3\ ^3D_1^o$	89961.46	0.70	4.12	3.05	0.03	0.97
8	$4s4p^3\ ^3D_2^o$	90094.34	-1.44	1.63	0.43	-0.80	0.98
9	$4s4p^3\ ^3D_3^o$	90667.75	2.03	3.46	1.97	-0.45	0.68
10	$4s4p^3\ ^3P_2^o$	104193.36	3.60	1.65	0.22	-1.68	0.00
11	$4s4p^3\ ^3P_0^o$	104255.04	12.99	9.68	4.40	0.02	-0.38
12	$4s4p^3\ ^3P_1^o$	104259.96	26.57	5.60	4.24	-0.42	0.31
13	$4s^24p4d\ ^1D_2^o$	110437.37	-3.60	0.53	0.29	-0.96	0.77
14	$4s^24p4d\ ^3F_2^o$	122090.91	11.96	7.78	5.61	3.30	4.65
15	$4s^24p4d\ ^3F_3^o$	123403.18	5.23	3.64	2.24	0.11	1.44
16	$4s^24p5s\ ^3P_0^o$	125041.82	11.00	12.09	10.54	7.12	6.89
17	$4s^24p5s\ ^3P_1^o$	125533.72	-8.85	-0.35	-0.76	-1.85	-0.15
18	$4s^24p4d\ ^3F_4^o$	125642.66	24.27	10.15	5.68	-1.13	-0.54
19	$4s^24p5s\ ^3P_2^o$	128936.75	-3.49	2.10	0.94	-1.81	-0.45
20	$4s^24p5s\ ^1P_1^o$	130591.07	-8.54	-1.33	-1.25	-2.15	-0.38
21	$4s^24p4d\ ^1P_1^o$	137565.08	13.92	6.19	4.15	1.53	3.00
22	$4s^24p4d\ ^3P_2^o$	139151.62	26.54	6.58	2.91	-0.94	0.38
23	$4s^24p4d\ ^3D_1^o$	139543.04	8.59	5.13	2.81	0.45	1.55
24	$4s^24p4d\ ^3P_1^o$	141784.77	6.64	5.01	3.11	1.05	2.69
25	$4s^24p4d\ ^3D_3^o$	141823.00	12.16	3.49	2.44	-0.03	1.29

Table 5. (continued)

No.	State	VV RCI	$\Delta E_{(\text{VV RCI (RSMBPT)})-(\text{VV RCI})}$				
			95%	99%	99.5%	99.95%	100%
26	$4s^24p4d\ ^3P_0^o$	141908.40	38.94	23.58	17.88	12.21	10.17
27	$4s^24p4d\ ^3D_2^o$	142329.40	15.47	5.73	4.33	1.29	2.82
28	$4s4p^3\ ^3S_1^o$	142728.82	10.36	6.44	5.07	-0.09	1.11
29	$4s^24p4d\ ^1F_3^o$	148254.58	33.45	10.95	5.85	2.92	3.60
30	$4s^24p5p\ ^1P_1$	149010.74	-8.20	1.30	0.89	-0.28	-0.47
31	$4s4p^3\ ^1D_2^o$	149337.81	17.88	6.20	4.28	0.90	2.54
32	$4s^24p5p\ ^3D_1$	151444.00	-9.52	2.16	0.40	-0.86	-0.49
33	$4s^24p5p\ ^3D_2$	151786.35	-12.39	0.23	-0.46	-1.82	-0.46
34	$4s^24p5p\ ^3P_0^o$	153156.20	-12.31	-1.03	-0.31	-0.87	-0.47
35	$4s^24p5p\ ^3P_1$	154556.08	-13.91	0.07	-0.40	-1.22	-0.52
36	$4s^24p5p\ ^3D_3$	154792.05	4.93	6.75	2.93	-0.11	-0.56
37	$4s^24p5p\ ^3P_2$	156058.57	-16.77	-1.48	-1.36	-1.92	-0.48
38	$4s^24p5p\ ^3S_1$	157478.90	-0.55	6.69	3.82	0.94	-0.56
39	$4s4p^3\ ^1P_1^o$	158678.10	26.45	8.49	5.33	0.72	1.88
40	$4s^24p5p\ ^1D_2$	159471.51	-13.02	-0.67	-0.87	-1.83	-0.34
41	$4s^24p5p\ ^1S_0$	165027.72	-1.67	2.69	0.97	-0.72	-0.49
42	$4s^24p6s\ ^3P_0^o$	185422.73	-0.79	6.18	5.72	3.98	4.50
43	$4s^24p6s\ ^3P_1^o$	185652.50	-13.70	-1.92	-1.80	-1.88	0.02
44	$4s^24p5d\ ^3F_2^o$	186497.20	-9.91	0.89	1.01	-0.64	0.89
45	$4s^24p5d\ ^3F_3^o$	187756.01	-11.57	-0.81	-1.29	-1.78	-0.19
46	$4s^24p4f\ ^1F_3$	187772.82	2.24	6.19	2.96	0.07	0.84
47	$4s^24p4f\ ^3F_3$	188094.45	1.68	1.21	1.20	-1.14	-0.24
48	$4s^24p4f\ ^3F_2$	188261.84	-4.91	0.21	0.90	-0.42	1.41
49	$4s^24p5d\ ^3D_2$	188357.90	-12.60	-2.21	-1.68	-2.05	-0.26
50	$4s^24p4f\ ^3F_4$	188358.89	-2.94	3.31	0.74	-1.71	-0.52
51	$4s^24p5d\ ^3D_1^o$	189181.95	-12.25	-2.03	-1.26	-1.11	0.64
52	$4s^24p6s\ ^3P_2^o$	189632.21	-7.87	0.09	0.06	-1.81	-0.34
53	$4s4p^{2\cdot}4P\ 4d\ ^3P_2$	189825.92	-17.91	-1.62	-2.00	-1.62	0.20
54	$4s^24p6s\ ^1P_1^o$	190303.32	-14.79	-2.77	-2.18	-2.05	-0.21
55	$4s^24p5d\ ^3F_4^o$	190692.95	-6.48	0.69	-0.09	-1.92	-0.57
56	$4s4p^{2\cdot}4P\ 4d\ ^5F_1$	191122.74	-12.03	0.36	0.23	-0.76	0.52
57	$4s^24p4f\ ^3G_3$	191415.95	2.29	5.36	3.66	0.85	1.55
58	$4s^24p5d\ ^1D_2^o$	191470.19	-13.06	-1.38	-0.87	-1.24	0.50
59	$4s4p^{2\cdot}4P\ 4d\ ^5F_2$	191604.93	-19.08	-1.68	-1.40	-1.55	0.34
60	$4s^24p4f\ ^3G_4$	191736.11	-14.11	1.67	1.57	-1.47	-0.37
61	$4s4p^{2\cdot}4P\ 4d\ ^3P_1$	191738.83	-3.89	1.40	-0.89	-1.54	-0.04
62	$4s^24p5d\ ^3D_3^o$	192143.31	-11.76	-1.12	-0.66	-1.46	0.20
63	$4s4p^{2\cdot}4P\ 4d\ ^5F_3$	192338.87	-16.26	-0.87	-0.47	-0.92	0.10
64	$4s4p^{2\cdot}4P\ 4d\ ^3P_0$	192422.20	-12.00	-1.54	-1.11	-1.52	-0.42
65	$4s^24p4f\ ^3G_5$	192463.15	12.30	10.95	5.33	-0.06	-0.53
66	$4s^24p5d\ ^3P_2^o$	192891.28	-12.17	-0.81	-0.75	-1.34	0.38
67	$4s^24p4f\ ^3D_3$	193006.39	1.65	2.31	1.20	-1.11	-0.40
68	$4s^24p5d\ ^3P_1^o$	193091.15	-8.90	2.03	1.11	-0.55	1.02

Table 5. (continued)

No.	State	VV RCI	$\Delta E_{(\text{VV RCI (RSMBPT)})-(\text{VV RCI})}$				
			95%	99%	99.5%	99.95%	100%
69	$4s^24p4f\ ^3D_2$	193261.09	-2.49	1.34	0.98	-0.70	0.94
70	$4s^24p5d\ ^3P_0^o$	193289.48	-0.40	4.21	3.18	1.84	2.26
71	$4s4p^2\ ^4P\ 4d\ ^5F_4$	193383.00	-17.47	-1.98	-1.29	-1.73	-0.23
72	$4s^24p4f\ ^1G_4$	193831.70	3.57	6.94	4.42	-1.02	-0.11
73	$4s^24p4f\ ^3D_1$	194065.96	3.71	2.07	1.79	-0.78	0.38
74	$4s^24p4f\ ^1D_2$	194417.51	-6.59	1.25	0.28	-2.13	-0.46
75	$4s4p^2\ ^4P\ 4d\ ^5F_5$	194813.38	-7.85	3.22	2.41	0.15	-0.47
76	$4s^24p5d\ ^1F_3^o$	195308.85	5.19	3.45	1.61	0.14	1.27
77	$4s^24p6p\ ^3D_1$	195326.09	-1.39	3.10	1.70	-0.45	-0.32
78	$4s^24p6p\ ^3P_1$	196089.89	-7.82	1.26	0.16	-1.46	-0.46
79	$4s^24p6p\ ^3D_2$	196363.01	-12.02	-0.72	-0.83	-2.19	-0.46
80	$4s^24p5d\ ^1P_1^o$	196449.92	-0.06	2.23	1.97	-0.32	1.09
81	$4s^24p6p\ ^3P_0$	196487.56	-11.57	-0.66	0.15	-1.21	-0.49
82	$4s4p^2\ ^4P\ 4d\ ^5D_0$	197575.86	-12.60	0.14	0.20	-1.06	0.16
83	$4s4p^2\ ^4P\ 4d\ ^5D_1$	197625.39	-14.48	-0.26	-0.13	-1.04	0.22
84	$4s4p^2\ ^4P\ 4d\ ^5D_2$	197799.40	-18.18	-1.91	-1.24	-1.67	0.14
85	$4s4p^2\ ^4P\ 4d\ ^5D_3$	198140.01	-10.09	0.29	0.53	-0.60	-0.06
86	$4s4p^2\ ^4P\ 4d\ ^5D_4$	198769.40	-11.27	-0.27	0.13	-1.24	-0.31
87	$4s^24p6p\ ^1P_1$	199127.90	-10.64	0.98	0.18	-1.43	-0.41
88	$4s4p^2\ ^4P\ 5s\ ^5P_1$	199434.62	-14.91	0.78	0.54	-1.67	-0.37
89	$4s^24p6p\ ^3P_2$	199670.12	-11.22	0.39	-0.72	-1.93	-0.34
90	$4s^24p6p\ ^3D_3$	199897.17	2.05	4.32	1.51	-0.96	-0.54
91	$4p^4\ ^1D_2$	200121.14	-3.80	8.54	3.98	-1.41	0.08
92	$4s^24p6p\ ^3S_1$	200722.94	-7.85	1.67	0.84	-0.65	-0.55
93	$4s4p^2\ ^4P\ 5s\ ^5P_2$	200855.25	-24.47	-2.05	-0.92	-2.23	-0.33
94	$4s^24p6p\ ^1D_2$	201357.48	-11.77	-0.23	-0.85	-2.04	-0.40
95	$4s4p^2\ ^4P\ 5s\ ^5P_3$	202670.04	-20.50	-1.74	-0.88	-1.59	-0.42
96	$4s^24p6p\ ^1S_0$	203344.68	-1.81	2.48	1.99	-0.75	-0.43
97	$4s4p^2\ ^4P\ 4d\ ^3F_2$	203981.62	5.51	18.23	15.65	-0.42	0.60
98	$4s4p^2\ ^4P\ 4d\ ^3F_3$	205082.24	20.97	16.09	15.70	4.22	0.44
99	$4s4p^2\ ^4P\ 4d\ ^3F_4$	206668.27	18.28	11.00	6.38	-0.20	0.18
100	$4s4p^2\ ^4P\ 5s\ ^3P_0$	207298.91	2.94	6.84	7.02	0.99	-0.04
101	$4s4p^2\ ^4P\ 5s\ ^3P_1$	208435.16	5.54	12.99	8.55	-1.06	-0.27
102	$4s4p^2\ ^4P\ 4d\ ^5P_3$	208999.03	-14.23	-1.19	-0.42	-0.99	-0.29
103	$4s4p^2\ ^4P\ 4d\ ^5P_2$	209605.76	-22.14	-2.30	-1.36	-1.56	0.22
104	$4s4p^2\ ^4P\ 4d\ ^5P_1$	210090.41	-17.96	-0.47	0.15	-0.34	0.56
105	$4s4p^2\ ^4P\ 5s\ ^3P_2$	210575.00	-3.50	5.52	2.09	-1.98	-0.16
N_{CSFs}		285503	176181	219451	232906	259552	274526

difference in the case of ‘100%’ is 10.17 cm^{-1} , and for the most levels, the difference between the VV RCI (RSMBPT) and VV RCI calculations do not reach 1 cm^{-1} .

4.2.2. Core-valence, core, core-core, and valence-valence correlations

Table 6 displays the total energies from the **CV+C+CC+VV RCI** calculations and the energy differences between the **CV+C+CC+VV RCI (RSMBPT)** and **CV+C+CC+VV RCI** calculations. For these computations including all electron correlations, as mentioned above, only the energy levels of the even configurations with $J = 0$ and the levels of the odd configurations with $J = 1$ are investigated. The calculations using the RSMBPT method are carried out in five steps, including 95, 99, 99.5, 99.95 and 100% of CV, C, CC and VV correlations. The results of the **CV+C+CC+VV RCI (RSMBPT)** in the case of ‘100%’ reproduce the regular GRASP2018 results. The largest difference between these results is 2.63E-05 a.u. (or 0.0000011%).

In Table 7, the energy levels from the calculations using the RSMBPT method (**CV+C+CC+VV RCI (RSMBPT)**) are compared. In the last line of the Table, the root-mean-square (rms) difference as compared with the results of regular GRASP2018 calculations (**CV+C+CC+VV RCI**) are given. When the most important K' configurations of CV, C, CC and VV correlations are progressively included in the calculations, the results converge to the results of the regular GRASP2018 calculations

and agree very well with them in the case of ‘100%’. The rms difference of the results is 1.90 cm⁻¹, and the largest difference between the results of these calculations is only up to 4.84 cm⁻¹. Omitting CSFs with a smaller impact of the CV, C, CC and VV correlations, the energy levels are still in good agreement with the regular computations, but the space of CSFs decreases significantly. For example, in the ‘99.5%’ case, the rms difference when comprising the **CV+C+CC+VV RCI** results is 94.63 cm⁻¹, while the space of CSFs decreases by a factor of 1.8 compared to the space in the **CV+C+CC+VV RCI** computations.

The presented results demonstrate that the RCI (RSMBPT) method works very well even when the MR set consists of orbitals with few different principal quantum numbers, namely with n , $n + 1$ and $n + 2$ (where $n = 4$). The results obtained using the RCI (RSMBPT) method agree very well with the regular GRASP2018 results in both computations when only VV and when all electron correlations are included. In addition, the RCI (RSMBPT) method works very well when the MR set consists of configurations with any orbital quantum numbers l , and with any shells occupation. Such studies have already been carried out in Refs. [4, 5] and confirmed in the present work.

Figure 3 displays the contribution of the included correlations (Δ_{cor}) using the **RCI (RSMBPT)**

Table 6. The total energies (in a.u.) from the **CV+C+CC+VV RCI** calculations and differences (in a.u.) between the **CV+C+CC+VV RCI (RSMBPT)** and **CV+C+CC+VV RCI** energies ($\Delta E_{(\text{CV+C+CC+VV RCI (RSMBPT)})-(\text{CV+C+CC+VV RCI})}$) for Se III are given when the CV, C, CC and VV correlations are included in the computations.

No.	State	CV+C+CC+VV RCI	$\Delta E_{(\text{CV+C+CC+VV RCI (RSMBPT)})-(\text{CV+C+CC+VV RCI})}$				
			95%	99%	99.5%	99.95%	100%
1	4s ² 4p ² ³ P ₀	-2426.0472568	0.0189950	0.0037583	0.0019239	0.0002134	0.0000042
2	4s ² 4p ² ¹ S ₀	-2425.9140952	0.0179700	0.0034686	0.0017785	0.0002033	0.0000018
3	4s4p ³ ³ D ₁ ^o	-2425.5492109	0.0149259	0.0029414	0.0014873	0.0001746	0.0000100
4	4s4p ³ ³ P ₁ ^o	-2425.4833650	0.0146271	0.0028168	0.0014096	0.0001598	0.0000076
5	4s ² 4p5s ³ P ₁ ^o	-2425.3866923	0.0144394	0.0026780	0.0013029	0.0001423	0.0000140
6	4s ² 4p5s ¹ P ₁ ^o	-2425.3632499	0.0141322	0.0025139	0.0012108	0.0001314	0.0000092
7	4s ² 4p5p ³ P ₀	-2425.3379284	0.0189785	0.0036897	0.0018012	0.0001797	0.0000040
8	4s4p ³ ¹ P ₁ ^o	-2425.3326795	0.0145635	0.0028397	0.0014578	0.0001992	0.0000183
9	4s ² 4p4d ³ D ₁ ^o	-2425.3215444	0.0145007	0.0028245	0.0014528	0.0002087	0.0000189
10	4s4p ³ ³ S ₁ ^o	-2425.3136899	0.0142691	0.0027807	0.0014103	0.0001843	0.0000141
11	4s ² 4p4d ³ P ₁ ^o	-2425.3074798	0.0143708	0.0027160	0.0013700	0.0001977	0.0000263
12	4s ² 4p5p ¹ S ₀	-2425.2811712	0.0188732	0.0036309	0.0017519	0.0001657	0.0000012
13	4s ² 4p4d ¹ P ₁ ^o	-2425.2300584	0.0145587	0.0028452	0.0014526	0.0001891	0.0000183

Table 6. (continued)

No.	State	CV+C+CC+VV RCI	$\Delta E_{(CV+C+CC+VV\ RCI\ (RSMBPT))-(CV+C+CC+VV\ RCI)}$				
			95%	99%	99.5%	99.95%	100%
14	$4s4p^2\ ^4P\ 4d\ ^3P_0$	-2425.1565596	0.0183315	0.0035864	0.0017834	0.0001845	0.0000022
15	$4s^24p6p\ ^3P_0$	-2425.1392487	0.0194013	0.0039494	0.0019745	0.0002050	0.0000045
16	$4s4p^2\ ^4P\ 4d\ ^5D_0$	-2425.1336409	0.0174931	0.0032964	0.0016133	0.0001691	0.0000054
17	$4s^24p6s\ ^3P_1^o$	-2425.1128679	0.0147355	0.0028337	0.0013878	0.0001399	0.0000142
18	$4s^24p6p\ ^1S_0$	-2425.1066908	0.0193385	0.0039076	0.0019286	0.0001819	0.0000011
19	$4s^24p5d\ ^3D_1^o$	-2425.0959911	0.0146767	0.0029321	0.0014872	0.0001649	0.0000112
20	$4s^24p6s\ ^1P_1^o$	-2425.0909697	0.0144467	0.0027629	0.0013389	0.0001358	0.0000095
21	$4s4p^2\ ^4P\ 5s\ ^3P_0$	-2425.0869795	0.0180387	0.0034797	0.0017028	0.0001766	0.0000033
22	$4s^24p5d\ ^3P_1^o$	-2425.0777530	0.0144899	0.0028563	0.0014218	0.0001554	0.0000105
23	$4s^24p5d\ ^1P_1^o$	-2425.0595874	0.0148405	0.0029726	0.0014743	0.0001577	0.0000099
N_{CSFs}		4456890	1011352	2055300	2438634	3317890	4341267

Table 7. The energy levels (in cm^{-1}) from the CV+C+CC+VV RCI calculations and differences (in cm^{-1}) between the CV+C+CC+VV RCI (RSMBPT) and CV+C+CC+VV RCI energies ($\Delta E_{(CV+C+CC+VV\ RCI\ (RSMBPT))-(CV+C+CC+VV\ RCI)}$) for Se III are given when the CV, C, CC and VV correlations are included in the computations.

No.	State	CV+C+CC+VV RCI	$\Delta E_{(CV+C+CC+VV\ RCI\ (RSMBPT))-(CV+C+CC+VV\ RCI)}$				
			95%	99%	99.5%	99.95%	100%
1	$4s^24p^2\ ^3P_0$	0	0	0	0	0	0
2	$4s^24p^2\ ^1S_0$	29225.6	-224.97	-63.59	-31.94	-2.23	-0.53
3	$4s4p^3\ ^3D_1^o$	109308.44	-893.06	-179.27	-95.84	-8.52	1.27
4	$4s4p^3\ ^3P_1^o$	123759.95	-958.66	-206.64	-112.88	-11.78	0.75
5	$4s^24p5s\ ^3P_1^o$	144977.15	-999.85	-237.09	-136.3	-15.61	2.17
6	$4s^24p5s\ ^1P_1^o$	150122.16	-1067.25	-273.1	-156.51	-18	1.12
7	$4s^24p5p\ ^3P_0$	155679.59	-3.63	-15.05	-26.93	-7.39	-0.04
8	$4s4p^3\ ^1P_1^o$	156831.60	-972.62	-201.61	-102.32	-3.13	3.1
9	$4s^24p4d\ ^3D_1^o$	159275.46	-986.39	-204.95	-103.41	-1.03	3.24
10	$4s4p^3\ ^3S_1^o$	160999.33	-1037.22	-214.55	-112.73	-6.39	2.18
11	$4s^24p4d\ ^3P_1^o$	162362.30	-1014.91	-228.77	-121.59	-3.47	4.84
12	$4s^24p5p\ ^1S_0$	168136.36	-26.74	-27.97	-37.76	-10.48	-0.65
13	$4s^24p4d\ ^1P_1^o$	179354.33	-973.66	-200.4	-103.45	-5.34	3.09
14	$4s4p^2\ ^4P\ 4d\ ^3P_0$	195485.44	-145.64	-37.73	-30.84	-6.36	-0.42
15	$4s^24p6p\ ^3P_0$	199284.75	89.16	41.94	11.09	-1.86	0.06
16	$4s4p^2\ ^4P\ 4d\ ^5D_0$	200515.51	-329.62	-101.36	-68.18	-9.73	0.28
17	$4s^24p6s\ ^3P_1^o$	205074.67	-934.87	-202.94	-117.67	-16.16	2.19
18	$4s^24p6p\ ^1S_0$	206430.38	75.38	32.76	1.02	-6.93	-0.66
19	$4s^24p5d\ ^3D_1^o$	208778.70	-947.76	-181.34	-95.86	-10.66	1.53
20	$4s^24p6s\ ^1P_1^o$	209880.76	-998.23	-218.46	-128.41	-17.04	1.17
21	$4s4p^2\ ^4P\ 5s\ ^3P_0$	210756.50	-209.89	-61.13	-48.53	-8.09	-0.19
22	$4s^24p5d\ ^3P_1^o$	212781.48	-988.76	-197.95	-110.2	-12.73	1.39
23	$4s^24p5d\ ^1P_1^o$	216768.39	-911.83	-172.45	-98.69	-12.23	1.25
N_{CSFs}		4456890	1011352	2055300	2438634	3317890	4341267
rms (in cm^{-1})			787.54	170.67	94.63	10.16	1.90

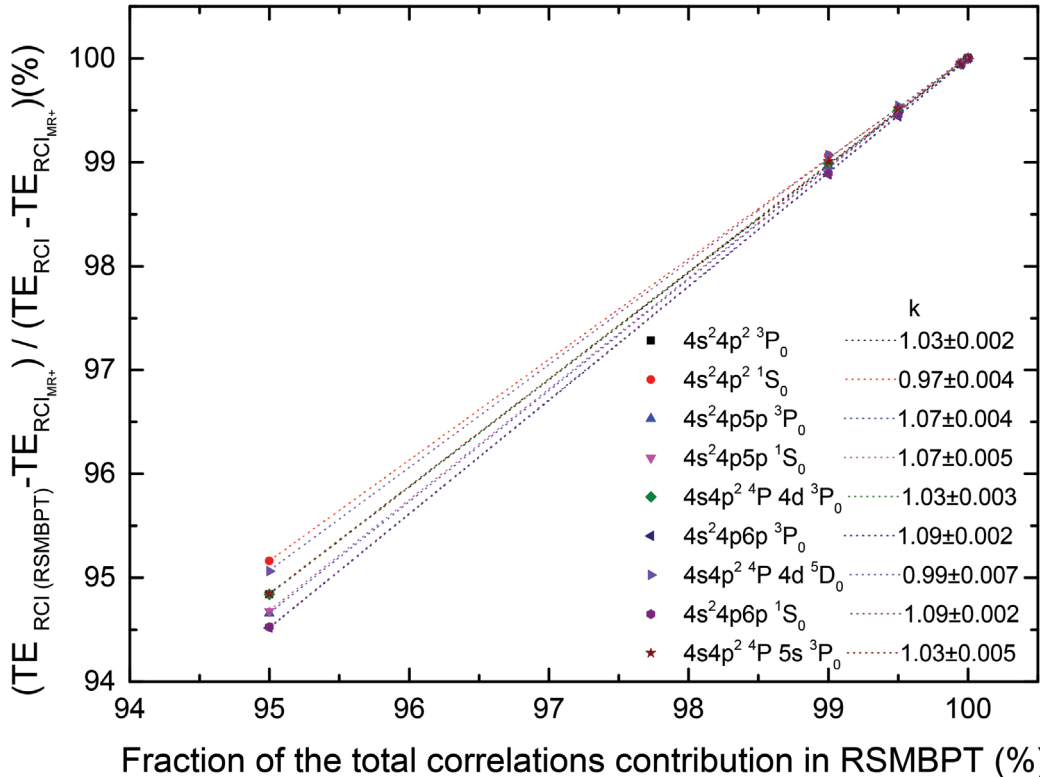


Fig. 3. Dependence of the contribution of included correlations (in the case of CV+C+CC+VV) on the specified fraction of the total correlations contribution used in the RCI (RSMBPT) method for the levels of even configurations.

method compared to the complete regular RCI computations, as a function of the specified fraction of the total correlations contribution used in the RCI (RSMBPT) method. This dependence is demonstrated for the levels of the even configurations with $J = 0$ in the case when the CV, C, CC and VV correlations are included. The contribution Δ_{cor} (in %) is computed according to the $(TE_{\text{RCI(RSMBPT)}} - TE_{\text{MR+}})/(TE_{\text{RCI}} - TE_{\text{MR+}})$, where TE represents the total energy from a certain computational scheme. $TE_{\text{RCI(RSMBPT)}}$ is the total energy from the RCI (RSMBPT) method using the specified fraction (in %) of the total correlations contribution. The results of MR+ are from the computations when the CSFs basis consists of the MR set together with the correlations which were not included using the RSMBPT method. As can be observed in the Figure, the computed Δ_{cor} is almost identical to the specified fraction (in %) of the total correlations contribution used in the RCI (RSMBPT) method, exhibiting a linear dependence. The linear fitting ($y = kx + a$) demonstrates that the slope coefficient (k) is approaching unity and that the error associated with the fitting itself is

negligible in comparison to the resulting value (see Fig. 3), indicating that the k factor is highly precise. Based on the above regularities, it can be said that by choosing the preferred amount of the correlations using the RSMBPT method, the error of the total energy (the difference of TE computed by incorporating 100% of the correlations and the reduced amount of the correlations) arising from the CSF basis reduction can be determined. Moreover, these regularities are stable for the configurations with different n , l , and shells occupation.

Table 8 presents the total energies from the MR+ and regular RCI computations when CV, C, CC and VV are included (CV+C+CC+VV RCI strategy). The Table also gives the calculated Δ_{cor} in %. All these results are given for the levels of the even configurations with $J = 0$ and for the levels of the odd configurations with $J = 1$. As can be seen from the Table, the computed contribution of the included correlations (Δ_{cor} in %) corresponds to the value which is used in the RCI (RSMBPT) method for all computed levels. By employing the linear dependence, it is feasible to ascertain not only the discrepancy in the total energy but also

Table 8. The total energies (in a.u.) from the **MR+** and regular **RCI** (when CV+C+CC+VV are included) computations are given. The column Δ_{cor} (in %) presents the contribution of included correlations using the **RCI (RSMBPT)** method compared to the regular **RCI** computations. The penultimate column in the Table shows the extrapolated total energy, and the last column shows the differences (in a.u.) between **CV+C+CC+VV RCI (RSMBPT)** in the case of ‘100%’ and the extrapolated value.

No.	State	TE		Δ_{cor}					TE	Diff
		MR+	RCI	95%	99%	99.5%	99.95%	100%		
1	$4s^24p^2\ ^3P_0$	-2425.6790685	-2426.0472568	94.841	98.979	99.477	99.942	99.999	-2426.0473077	0.0000551
2	$4s^24p^2\ ^1S_0$	-2425.5428084	-2425.9140952	95.160	99.066	99.521	99.945	100.000	-2425.9142520	0.0001585
7	$4s^24p5p\ ^3P_0$	-2424.9826929	-2425.3379284	94.657	98.961	99.493	99.949	99.999	-2425.3380609	0.0001365
12	$4s^24p5p\ ^1S_0$	-2424.9265608	-2425.2811712	94.678	98.976	99.506	99.953	100.000	-2425.2813509	0.0001809
14	$4s4p^2\ ^4P\ 4d\ ^3P_0$	-2424.8013581	-2425.1565596	94.839	98.990	99.498	99.948	99.999	-2425.1566595	0.0001021
15	$4s^24p6p\ ^3P_0$	-2424.7852302	-2425.1392487	94.520	98.884	99.442	99.942	99.999	-2425.1391623	-0.0000819
16	$4s4p^2\ ^4P\ 4d\ ^5D_0$	-2424.7793276	-2425.1336409	95.063	99.070	99.545	99.952	99.998	-2425.1338937	0.0002582
18	$4s^24p6p\ ^1S_0$	-2424.7533700	-2425.1066908	94.527	98.894	99.454	99.949	100.000	-2425.1066409	-0.0000488
21	$4s4p^2\ ^4P\ 5s\ ^3P_0$	-2424.7371032	-2425.0869795	94.844	99.005	99.513	99.950	99.999	-2425.0871396	0.0001633
3	$4s4p^3\ ^3D_1^o$	-2425.2697629	-2425.5492109	94.659	98.947	99.468	99.938	99.996	-2425.5492656	0.0000647
4	$4s4p^3\ ^3P_1^o$	-2425.2000921	-2425.4833650	94.836	99.006	99.502	99.944	99.997	-2425.4835008	0.0001434
5	$4s^24p5s\ ^3P_0^o$	-2425.1080919	-2425.3866923	94.817	99.039	99.532	99.949	99.995	-2425.3869547	0.0002764
6	$4s^24p5s\ ^1P_0^o$	-2425.0839277	-2425.3632499	94.941	99.100	99.567	99.953	99.997	-2425.3636406	0.0003999
8	$4s4p^3\ ^1P_1^o$	-2425.0483337	-2425.3326795	94.878	99.001	99.487	99.930	99.994	-2425.3327708	0.0001096
9	$4s^24p4d\ ^3D_1^o$	-2425.0429675	-2425.3215444	94.795	98.986	99.478	99.925	99.993	-2425.3216390	0.0001134
10	$4s4p^3\ ^3S_1^o$	-2425.0277709	-2425.3136899	95.009	99.027	99.507	99.936	99.995	-2425.3137813	0.0002757
11	$4s^24p4d\ ^3P_1^o$	-2425.0328347	-2425.3074798	94.768	99.011	99.501	99.928	99.990	-2425.3076775	0.0002240
13	$4s^24p4d\ ^1P_1^o$	-2424.9528259	-2425.2300584	94.749	98.974	99.476	99.932	99.993	-2425.2301416	0.0001015
17	$4s^24p6s\ ^3P_0^o$	-2424.8346996	-2425.1128679	94.703	98.981	99.501	99.950	99.995	-2425.1130097	0.0001560
19	$4s^24p5d\ ^3D_1^o$	-2424.8185077	-2425.0959911	94.711	98.943	99.464	99.941	99.996	-2425.0959952	0.0000152
20	$4s^24p6s\ ^1P_1^o$	-2424.8135056	-2425.0909697	94.793	99.004	99.517	99.951	99.997	-2425.0911278	0.0001675
22	$4s^24p5d\ ^3P_1^o$	-2424.8008383	-2425.0777530	94.767	98.969	99.487	99.944	99.996	-2425.0778051	0.0000626
23	$4s^24p5d\ ^1P_1^o$	-2424.7839472	-2425.0595874	94.616	98.922	99.465	99.943	99.996	-2425.0595818	0.0000043

the value of the total energy itself. By taking results only from smaller bases that include 95 and 99% of correlations using the RSMBPT method, it is possible to extrapolate the total energy value that would have been obtained if 100% of the correlations would be included. This could be very important for the study of energy levels that are close to each other. These extrapolated values and the differences with the total energies computed by incorporating 100% of the correlations using the RSMBPT method are given in Table 8 (last two columns, respectively). The differences in the last column of the Table are small and reach up to 3.9E-04 a.u. (or 0.000016%). One of the reasons of the disagreement could be the fact that while using the RSMBPT method the impact of off-diagonal matrix ele-

ments is not taken into account. Similar computations were performed without the Breit and QED effects, and the trends of the results are the same. Table 9 presents the total energies from the regular **CV+C+CC+VV RCI**, differences between **CV+C+CC+VV RCI (RSMBPT)**, **CV+C+CC+VV RCI (accum)** and the **CV+C+CC+VV RCI** calculations. The results in the columns $\Delta E_{(\text{CV+C+CC+VV RCI (accum)})-(\text{CV+C+CC+VV RCI})}$ present the results from the ‘rmixaccumulate’ program (which is included in the GRASP package). This program accumulates the dominating CSFs by mixing coefficients up to a user defined fraction of the atomic state function. In the Table, few different values to accumulate the CSF basis are taken as an example. In the last lines of the Table, the number of CSFs, the rms,

Table 9. The total energies (in a.u.) from the **CV+C+CC+VV RCI** calculations and differences (in a.u.) between the **CV+C+CC+VV RCI (RSMBPT)** and **CV+C+CC+VV RCI** energies ($\Delta E_{(\text{CV+C+CC+VV RCI (RSMBPT)})-(\text{CV+C+CC+VV RCI})}$) and between the **CV+C+CC+VV RCI (accum)** and **CV+C+CC+VV RCI** energies ($\Delta E_{(\text{CV+C+CC+VV RCI (accum)})-(\text{CV+C+CC+VV RCI})}$) for Se III are given when the CV, C, CC and VV correlations are included in the computations.

No.	State	CV+C+CC+VV RCI	$\Delta E_{(\text{CV+C+CC+VV RCI (RSMBPT)})-(\text{CV+C+CC+VV RCI})}$				
			95%	99%	99.5%	99.95%	100%
1	$4s^24p^2\ ^3P_0$	-2426.0472568	0.0189950	0.0037583	0.0019239	0.0002134	0.0000042
2	$4s^24p^2\ ^1S_0$	-2425.9140952	0.0179700	0.0034686	0.0017785	0.0002033	0.0000018
3	$4s^24p5p\ ^3P_0$	-2425.3379284	0.0189785	0.0036897	0.0018012	0.0001797	0.0000040
4	$4s^24p5p\ ^1S_0$	-2425.2811712	0.0188732	0.0036309	0.0017519	0.0001657	0.0000012
5	$4s4p^2\ ^4P\ 4d\ ^3P_0$	-2425.1565596	0.0183315	0.0035864	0.0017834	0.0001845	0.0000022
6	$4s^24p6p\ ^3P_0$	-2425.1392487	0.0194013	0.0039494	0.0019745	0.0002050	0.0000045
7	$4s4p^2\ ^4P\ 4d\ ^5D_0$	-2425.1336409	0.0174931	0.0032964	0.0016133	0.0001691	0.0000054
8	$4s^24p6p\ ^1S_0$	-2425.1066908	0.0193385	0.0039076	0.0019286	0.0001819	0.0000011
9	$4s4p^2\ ^4P\ 5s\ ^3P_0$	-2425.0869795	0.0180387	0.0034797	0.0017028	0.0001766	0.0000033
N_{CSFs}		1303883	298310	598587	711815	978504	1275596
rms (in a.u.)			0.0186129	0.0036463	0.0018098	0.0001872	0.0000034
ΔE_{max} (in a.u.)			0.0194013	0.0039494	0.0019745	0.0002134	0.0000054
ΔE_{min} (in a.u.)			0.0174931	0.0032964	0.0016133	0.0001657	0.0000011
No.	State	CV+C+CC+VV RCI	$\Delta E_{(\text{CV+C+CC+VV RCI (accum)})-(\text{CV+C+CC+VV RCI})}$				
			0.99947	0.9995	0.9997	0.99982	0.99996
1	$4s^24p^2\ ^3P_0$	-2426.0472568	0.0023977	0.0022523	0.0012670	0.0007436	0.0001736
2	$4s^24p^2\ ^1S_0$	-2425.9140952	0.0020293	0.0018963	0.0009976	0.0005485	0.0001113
3	$4s^24p5p\ ^3P_0$	-2425.3379284	0.0038803	0.0036183	0.0019734	0.0010759	0.0002032
4	$4s^24p5p\ ^1S_0$	-2425.2811712	0.0054104	0.0050714	0.0028190	0.0015648	0.0002892
5	$4s4p^2\ ^4P\ 4d\ ^3P_0$	-2425.1565596	0.0152710	0.0145833	0.0094772	0.0059936	0.0014514
6	$4s^24p6p\ ^3P_0$	-2425.1392487	0.0064461	0.0059563	0.0031491	0.0017466	0.0003503
7	$4s4p^2\ ^4P\ 4d\ ^5D_0$	-2425.1336409	0.0195031	0.0184791	0.0116459	0.0072768	0.0017522
8	$4s^24p6p\ ^1S_0$	-2425.1066908	0.0067823	0.0063778	0.0037588	0.0021983	0.0004530
9	$4s4p^2\ ^4P\ 5s\ ^3P_0$	-2425.0869795	0.0125242	0.0117847	0.0071323	0.0042394	0.0008940
N_{CSFs}		1303883	211374	217926	278203	342510	539460
rms (in a.u.)			0.0100674	0.0095258	0.0059142	0.0036391	0.0008480
ΔE_{max} (in a.u.)			0.0195031	0.0184791	0.0116459	0.0072768	0.0017522
ΔE_{min} (in a.u.)			0.0020293	0.0018963	0.0009976	0.0005485	0.0001113

the largest (ΔE_{max}) and the smallest (ΔE_{min}) differences with the results of the regular GRASP2018 calculations (**CV+C+CC+VV RCI**) are given for each computation. As seen from the Table, the differences between **CV+C+CC+VV RCI (RSMBPT)** and **CV+C+CC+VV RCI** are similar for all levels and there is almost no scatter in the results with the same fraction of the total correlations contribution used in the RSMBPT method. For example, in the ‘95%’ case, the rms is equal to 0.0186129, ΔE_{max} is 0.0194013 and ΔE_{min} is 0.0174931. Comparing

the **CV+C+CC+VV RCI (accum)** results with **CV+C+CC+VV RCI**, the change in total energies for all levels is different in the same calculation using the ‘rmixaccumulate’ program. For example, in the ‘0.99947’ case, the rms is equal to 0.0100674, ΔE_{max} is 0.0195031 and ΔE_{min} is 0.0020293. Finding the analogous calculation for **CV+C+CC+VV RCI (RSMBPT)** and **CV+C+CC+VV RCI (accum)** is quite complex since using RSMBPT the selection process is based on configurations, meanwhile the ‘rmixaccumulate’ program is based on CSFs.

It should be mentioned that in both computations only CSFs with non-zero matrix elements in the sets of spin-angular integration with the CSFs belonging to the configurations in the MR are included. Thus, performing the **CV+C+CC+VV RCI (RSMBPT)** computations firstly, the RSMBPT procedure, which is based on configurations, was applied and after the reductions of CSFs basis was done based on CSFs. For example, two computations **CV+C+CC+VV RCI (RSMBPT)** and **CV+C+CC+VV RCI (accum)** have a similar rms deviation with the regular RCI computation 0.0036463 in the case of 99% using RSMBPT, and 0.0036391 in the case of the ‘rmixaccumulate’ program with a fraction equal to 0.99982. The similar largest difference with the regular RCI computation is 0.0194013 in the case of 95% using RSMBPT, and 0.0195031 in the case of the ‘rmixaccumulate’ program with a fraction equal to 0.99947. But the min value and rms are very different.

The transition properties of E1 transitions between the levels of the even configurations with $J = 0$ and the levels of the odd configurations with $J = 1$ are also computed. The calculations are done in a regular way without and with the accumulation option and using the RSMBPT method when CV, C, CC and VV are included. Table 10 shows the comparison of the line strengths, cancellation factors (CF) [35], $G_{S=0}$ parameters, and the estimated accuracy for few E1 transitions using different computational schemes. The uncertainties of the line strengths obtained in this work are estimated based on the quantitative and qualitative evaluation (QQE) method described in Refs. [32–34]. By comparing the line strengths from the regular GRASP2018 with the results from the **CV+C+CC+VV RCI (RSMBPT)** calculations in the case of ‘100%’, it is seen that the results using RSMBPT are reproduced. Excluding the CV, C, CC and VV correlations with the smallest im-

Table 10. Comparison of the computed wavelengths (λ in Å), line strengths (S in a.u.), cancellation factors, CF and the $G_{S=0}$ parameters using different strategies. Subscript B means the Babushkin gauge, and C is the Coulomb gauge. The name of the computational scheme **CV+C+CC+VV RCI (accum)** is marked as **RCI (accum)**, and the **CV+C+CC+VV RCI(RSMBPT)** is marked as **RCI (RSMBPT)** in the Table.

Strategy	λ	S_B	S_C	CF_B	CF_C	$G_{S=0}$	Acc.
$4s4p^3\ ^3D_1^o - 4s4p^2\ ^4P\ 5s\ ^3P_0$							
CV+C+CC+VV RCI	985.73	6.29208E-01	1.00321E+00	2.24E-01	2.42E-01	6.79773E+00	D+
RCI (accum) 0.99996	985.37	6.32634E-01	1.00671E+00	2.26E-01	2.44E-01	6.82291E+00	D+
RCI (accum) 0.99982	983.59	6.43904E-01	1.01617E+00	2.32E-01	2.49E-01	6.93329E+00	D+
RCI (accum) 0.9997	981.89	6.51795E-01	1.01997E+00	2.37E-01	2.52E-01	7.04982E+00	D+
RCI (accum) 0.9995	979.31	6.62218E-01	1.02468E+00	2.44E-01	2.58E-01	7.24111E+00	D+
RCI (accum) 0.99947	978.85	6.63737E-01	1.02502E+00	2.43E-01	2.57E-01	7.21203E+00	D+
RCI (RSMBPT) 100%	985.74	6.29174E-01	1.00326E+00	2.23E-01	2.42E-01	6.79638E+00	D+
RCI (RSMBPT) 99.95%	985.72	6.29329E-01	1.00362E+00	2.24E-01	2.42E-01	6.79487E+00	D+
RCI (RSMBPT) 99.5%	985.27	6.27428E-01	1.00053E+00	2.24E-01	2.42E-01	6.79565E+00	D+
RCI (RSMBPT) 99%	984.58	6.25883E-01	9.97199E-01	2.23E-01	2.43E-01	6.80689E+00	D+
RCI (RSMBPT) 95%	979.13	6.19460E-01	9.74757E-01	2.21E-01	2.44E-01	6.97288E+00	D+
$4s4p^3\ ^3D_1^o - 4s^24p6p\ ^3P_0$							
CV+C+CC+VV RCI	1111.40	1.97065E-01	2.18151E-01	8.30E-02	6.41E-02	2.85371E+01	B
RCI (accum) 0.99996	1112.43	2.00373E-01	2.21194E-01	8.35E-02	6.39E-02	2.93229E+01	B
RCI (accum) 0.99982	1115.45	2.09708E-01	2.30566E-01	7.76E-02	5.67E-02	3.05418E+01	B
RCI (accum) 0.9997	1117.34	2.18585E-01	2.40375E-01	6.97E-02	4.84E-02	3.04770E+01	B
RCI (accum) 0.9995	1119.05	2.33846E-01	2.58968E-01	5.51E-02	3.48E-02	2.84319E+01	B
RCI (accum) 0.99947	1119.13	2.35264E-01	2.60959E-01	5.29E-02	3.48E-02	2.84319E+01	B

Table 10. (continued)

Strategy	λ	S_B	S_C	CF_B	CF_C	$G_{S=0}$	Acc.
RCI (RSMBPT) 100%	1111.42	1.97088E-01	2.18166E-01	8.30E-02	6.41E-02	2.85512E+01	B
RCI (RSMBPT) 99.95%	1111.32	1.97034E-01	2.18063E-01	8.30E-02	6.41E-02	2.86052E+01	B
RCI (RSMBPT) 99.5%	1110.08	1.95504E-01	2.16309E-01	8.18E-02	6.32E-02	2.86824E+01	B
RCI (RSMBPT) 99%	1108.68	1.93800E-01	2.13872E-01	8.05E-02	6.22E-02	2.94122E+01	B
RCI (RSMBPT) 95%	1099.40	1.82939E-01	1.99521E-01	7.21E-02	5.58E-02	3.33109E+01	B
$4s^24p5s\ ^3P_1^o - 4s^24p6p\ ^1S_0$							
CV+C+CC+VV RCI	1627.25	9.69183E-03	9.28846E-03	7.98E-03	4.28E-03	-6.58296E+01	B+
RCI (accum) 0.99996	1626.84	9.43809E-03	8.82439E-03	7.91E-03	4.19E-03	-4.13651E+01	B+
RCI (accum) 0.99982	1625.28	8.68898E-03	7.58237E-03	7.73E-03	3.94E-03	-2.00631E+01	C+
RCI (accum) 0.9997	1624.30	8.17001E-03	6.80147E-03	7.61E-03	3.79E-03	-1.47317E+01	C
RCI (accum) 0.9995	1622.91	7.44070E-03	5.82335E-03	7.36E-03	3.55E-03	-1.08477E+01	D+
RCI (accum) 0.99947	1622.66	7.33234E-03	5.67099E-03	7.32E-03	3.51E-03	-1.03166E+01	D+
RCI (RSMBPT) 100%	1627.33	9.69344E-03	9.28389E-03	7.98E-03	4.28E-03	-6.48160E+01	B+
RCI (RSMBPT) 99.95%	1627.02	9.68893E-03	9.19334E-03	7.99E-03	4.26E-03	-5.31666E+01	B+
RCI (RSMBPT) 99.5%	1623.63	9.70334E-03	8.94842E-03	7.96E-03	4.16E-03	-3.42194E+01	B
RCI (RSMBPT) 99%	1620.14	9.69110E-03	8.92997E-03	7.90E-03	4.15E-03	-3.38773E+01	B
RCI (RSMBPT) 95%	1599.27	9.83055E-03	7.95396E-03	7.78E-03	3.75E-03	-1.26580E+01	C
$4s^24p5p\ ^1S_0 - 4s^24p5d\ ^1P_1^o$							
CV+C+CC+VV RCI	2056.26	1.28936E+01	6.02123E+00	4.82E-01	3.37E-01	-3.05221E+00	E
RCI (accum) 0.99996	2050.73	1.28697E+01	5.98194E+00	4.83E-01	3.38E-01	-3.02977E+00	E
RCI (accum) 0.99982	2035.90	1.28063E+01	5.87452E+00	4.84E-01	3.41E-01	-2.96810E+00	E
RCI (accum) 0.9997	2025.87	1.27665E+01	5.80378E+00	4.84E-01	3.43E-01	-2.92718E+00	E
RCI (accum) 0.9995	2011.53	1.27078E+01	5.69493E+00	4.85E-01	3.45E-01	-2.86398E+00	E
RCI (accum) 0.99947	2009.55	1.26997E+01	5.68012E+00	4.85E-01	3.45E-01	-2.85547E+00	E
RCI (RSMBPT) 100%	2056.18	1.28927E+01	6.02228E+00	4.82E-01	3.37E-01	-3.05342E+00	E
RCI (RSMBPT) 99.95%	2056.33	1.28920E+01	6.02323E+00	4.82E-01	3.38E-01	-3.05445E+00	E
RCI (RSMBPT) 99.5%	2058.84	1.28848E+01	6.02658E+00	4.82E-01	3.39E-01	-3.05982E+00	E
RCI (RSMBPT) 99%	2062.39	1.28808E+01	6.04391E+00	4.83E-01	3.40E-01	-3.07530E+00	E
RCI (RSMBPT) 95%	2094.38	1.28651E+01	6.19306E+00	4.82E-01	3.43E-01	-3.20467E+00	E
$4s^24p^2\ ^3P_0 - 4s4p^3\ ^3D_1^o$							
CV+C+CC+VV RCI	914.84	1.34217E-01	1.02639E-01	1.74E-02	8.49E-03	-9.85309E+00	D+
RCI (accum) 0.99996	913.83	1.34955E-01	1.02857E-01	1.75E-02	8.53E-03	-9.72275E+00	D+
RCI (accum) 0.99982	910.29	1.36953E-01	1.03277E-01	1.78E-02	8.63E-03	-9.33166E+00	D+
RCI (accum) 0.9997	907.44	1.38392E-01	1.03355E-01	1.79E-02	8.69E-03	-8.99907E+00	D+
RCI (accum) 0.9995	903.05	1.40476E-01	1.03508E-01	1.82E-02	8.80E-03	-8.57272E+00	D+
RCI (accum) 0.99947	902.38	1.40770E-01	1.03504E-01	1.82E-02	8.81E-03	-8.50874E+00	D+
RCI (RSMBPT) 100%	914.83	1.34206E-01	1.02620E-01	1.74E-02	8.48E-03	-9.84897E+00	D+
RCI (RSMBPT) 99.95%	914.91	1.34091E-01	1.02576E-01	1.74E-02	8.49E-03	-9.86616E+00	D+
RCI (RSMBPT) 99.5%	915.65	1.33498E-01	1.02287E-01	1.74E-02	8.47E-03	-9.92974E+00	D+
RCI (RSMBPT) 99%	916.35	1.33157E-01	1.02251E-01	1.74E-02	8.47E-03	-1.00183E+01	D+
RCI (RSMBPT) 95%	922.38	1.32410E-01	1.05113E-01	1.74E-02	8.73E-03	-1.15580E+01	D+

Table 10. (continued)

Strategy	λ	S_B	S_C	CF_B	CF_C	$G_{S=0}$	Acc.
$4s^24p^2\ ^3P_0 - 4s^24p4d\ ^3D_1^o$							
CV+C+CC+VV RCI	627.84	6.14607E+00	4.71096E+00	4.17E-01	3.94E-01	-9.94495E+00	D+
RCI (accum) 0.99996	627.45	6.14926E+00	4.70313E+00	4.18E-01	3.94E-01	-9.85846E+00	D+
RCI (accum) 0.99982	626.04	6.15669E+00	4.67532E+00	4.21E-01	3.97E-01	-9.58524E+00	D+
RCI (accum) 0.9997	624.87	6.15789E+00	4.64922E+00	4.24E-01	3.98E-01	-9.37375E+00	D+
RCI (accum) 0.9995	623.02	6.15485E+00	4.60592E+00	4.27E-01	4.01E-01	-9.06659E+00	D+
RCI (accum) 0.99947	622.75	6.15570E+00	4.60079E+00	4.28E-01	4.01E-01	-9.02472E+00	D+
RCI (RSMBPT) 100%	627.83	6.14447E+00	4.70959E+00	4.17E-01	3.93E-01	-9.94365E+00	D+
RCI (RSMBPT) 99.95%	627.85	6.14266E+00	4.70825E+00	4.17E-01	3.93E-01	-9.94412E+00	D+
RCI (RSMBPT) 99.5%	628.25	6.14983E+00	4.72028E+00	4.18E-01	3.94E-01	-9.99964E+00	D+
RCI (RSMBPT) 99%	628.65	6.15474E+00	4.72978E+00	4.18E-01	3.95E-01	-1.00488E+01	D+
RCI (RSMBPT) 95%	631.76	6.15534E+00	4.78122E+00	4.19E-01	4.01E-01	-1.05039E+01	D+

pact (cases 99.95, 99.5 and 99 in Table 10), we see that the line strengths almost do not change compared to the results when all these correlations are included. From Table 10 we also see that CFs in both (Babushkin and Coulomb) gauges are stable when the most important configurations of CV, C, CC and VV correlations in a different amount are included. Comparing the line strengths from the regular GRASP2018 with the results from the **CV+C+CC+VV RCI (accum)** calculations, it is seen that the results agree among themselves but the differences with **CV+C+CC+VV RCI** are larger than those obtained with **CV+C+CC+VV RCI (RSMBPT)**.

5. Conclusions

The method, based on the Rayleigh–Schrödinger perturbation theory in an irreducible tensorial form, is extended to estimate the VV correlations. The expressions to calculate the influence of these correlations are provided. This extended RSMBPT method allows one to estimate the contribution of any K' configuration of the CV, C, CC and VV correlations with the preferred core, virtual orbitals sets and with any number of valence electrons for any atom or ion.

The developed RCI (RSMBPT) method works perfectly when the CV, C, CC and VV correlations are taken into account using the RSMBPT method, and the results reproduce the regular GRASP2018 data. Also, this method works very well even when the MR set consists of orbitals with few different

principal quantum numbers, namely with n , $n + 1$ and $n + 2$ (where $n = 4$). The main advantages of the developed method in comparison to the regular method are as follows: it allows one to identify the most important CV, C, CC and VV correlations and significantly reduces the CSF space. These benefits of the RSMBPT method over the regular method would be helpful and valuable for calculations involving complex atoms and ions.

By employing the RSMBPT method to analyze only the results of smaller bases, for example, with 95 and 99% correlations, it is possible to extrapolate very accurately the total value of the energy that would be obtained by including 100% of the correlations. The extrapolation of the total energies would be helpful for complex computations when considering CV, C, CC and VV correlations, as such computations lead to a large CSFs basis and are time consuming. This could be very important for the study of energy levels that are close to each other.

Comparing the **CV+C+CC+VV RCI (RSMBPT)** and **CV+C+CC+VV RCI (accum)** results with the regular **CV+C+CC+VV RCI** results, the differences between the results using RSMBPT and the regular GRASP2018 energies are similar for all computed levels, while the differences between the results using the ‘rmixaccumulate’ program and the regular ones are scattering for all levels. The reduction of CSFs basis in both computations is different, the selection process in RSMBPT is based on configurations, and meanwhile the ‘rmixaccumulate’ program is based on CSFs.

Most theoretical methods have a CI or RCI stage. It is usually at this stage that the size of the CSF base in terms of computing capacity is decided. Due to the complexity of the computation, a usually restricted active space (RAS) approach is used, which is then further reduced on the basis of one or the other theoretical principles. Regular GRASP2018 calculations also use the RAS approach, and it will be reduced later using the ‘rmixaccumulate’, ‘rcsfinteract’ and ‘cndens’ programs [11, 36]. How these or other RAS reduction mechanisms work for the total energy TE, and what kind of error can be expected, can only be known after a full study. Meanwhile, using the RSMBPT correlation selection method to reduce the RAS space, we also determine the resulting TE error (the difference of TE computed in full RAS and reduced RAS) created by the RAS space reduction. To our knowledge, this theoretical method is the only one that allows us to predict the errors of reduction of the RAS to the TE on the basis of the calculation parameters.

References

- [1] P. Jönsson, G. Gaigalas, J. Bieroń, C. Froese Fischer, and I.P. Grant, New version: GRASP2K relativistic atomic structure package, *Comput. Phys. Commun.* **184**(9), 2197–2203 (2013), <https://doi.org/10.1016/j.cpc.2013.02.016>
- [2] C. Froese Fischer, G. Gaigalas, P. Jönsson, and J. Bieroń, GRASP2018—A Fortran 95 version of the General Relativistic Atomic Structure Package, *Comput. Phys. Commun.* **237**, 184–187 (2019), <https://doi.org/10.1016/j.cpc.2018.10.032>
- [3] G. Gaigalas, P. Rynkun, and L. Kitovienė, Second-order Rayleigh–Schrödinger perturbation theory for the GRASP2018 package: Core–valence correlations, *Lith. J. Phys.* **64**(1), 20–39 (2024), <https://doi.org/10.3952/physics.2024.64.1.3>
- [4] G. Gaigalas, P. Rynkun, and L. Kitovienė, Second-order Rayleigh–Schrödinger perturbation theory for the GRASP2018 package: Core correlations, *Lith. J. Phys.* **64**(2), 73–81 (2024), <https://doi.org/10.3952/physics.2024.64.2.1>
- [5] G. Gaigalas, P. Rynkun, and L. Kitovienė, Second-order Rayleigh–Schrödinger perturbation theory for the GRASP2018 package: Core–core correla-
- tions, *Lith. J. Phys.* **64**(3), 139–161 (2024), <https://doi.org/10.3952/physics.2024.64.3.1>
- [6] P. Jönsson, M. Godefroid, G. Gaigalas, J. Ekman, J. Grumer, W. Li, J. Li, T. Brage, I.P. Grant, J. Bieroń, and C. Froese Fischer, An introduction to relativistic theory as implemented in GRASP, *Atoms* **11**(1), 7 (2023), <https://doi.org/10.3390/atoms11010007>
- [7] I. Lindgren and J. Morrison, *Atomic Many-body Theory* (Springer-Verlag Berlin Heidelberg, New York, 1982).
- [8] I. Hubač and S. Wilson, *Brillouin–Wigner Methods for Many-body Systems* (Springer Dordrecht Heidelberg London New York, 2010), <https://doi.org/10.1007/978-90-481-3373-4>
- [9] S. Gustafsson, P. Jönsson, C. Froese Fischer, and I.P. Grant, Combining multiconfiguration and perturbation methods: perturbative estimates of core–core electron correlation contributions to excitation energies in Mg-like iron, *Atoms* **5**(1), 3 (2017), <https://doi.org/10.3390/atoms5010003>
- [10] G. Gaigalas, P. Rynkun, L. Radžiūtė, D. Kato, M. Tanaka, and P. Jönsson, Energy level structure and transition data of Er^{2+} , *Astrophys. J. Suppl. Ser.* **248**, 13 (2020), <https://doi.org/10.3847/1538-4365/ab881a>
- [11] P. Jönsson, G. Gaigalas, Ch.F. Fischer, J. Bieroń, I.P. Grant, T. Brage, J. Ekman, M. Godefroid, J. Grumer, J. Li, and W. Li, GRASP manual for users, *Atoms* **11**(4), 68 (2023), <https://doi.org/10.3390/atoms11040068>
- [12] G. Merkelis, G. Gaigalas, and Z. Rudzikas, Irreducible tensorial form of the effective Hamiltonian of an atom and the diagrammatic representation in the first two orders of the stationary perturbation theory, *Liet. Fiz. Rink. (Sov. Phys. Coll.)* **25**, 14–31 (1985) [in Russian].
- [13] G. Merkelis, G. Gaigalas, J.G. Kaniauskas, and Z. Rudzikas, Application of the graphical method of the angular momentum theory to the study of the stationary perturbation series, *Izvest. Acad. Nauk SSSR, Phys. Coll.* **50**, 1403–1410 (1986) [in Russian].
- [14] G. Gaigalas, *Irreducible Tensorial Form of the Stationary Perturbation Theory for Atoms and*

- Ions with Open Shells*, PhD Thesis (Institute of Physics, Vilnius, 1989), <https://kolekcijos.biblioteka.vu.lt/en/objects/990007058341008452#00001> [in Russian].
- [15] G. Racah, Theory of complex spectra. I, Phys. Rev. **61**, 186 (1942), <https://doi.org/10.1103/PhysRev.61.186>
- [16] G. Racah, Theory of complex spectra. II, Phys. Rev. **62**, 438 (1942), <https://doi.org/10.1103/PhysRev.62.438>
- [17] G. Racah, Theory of complex spectra. III, Phys. Rev. **63**, 367 (1943), <https://doi.org/10.1103/PhysRev.63.367>
- [18] G. Racah, Theory of complex spectra. IV, Phys. Rev. **76**, 1352 (1949), <https://doi.org/10.1103/PhysRev.76.1352>
- [19] Z.B. Rudzikas, *Theoretical Atomic Spectroscopy* (Cambridge University Press, Cambridge, 1997).
- [20] Z.B. Rudzikas and J.M. Kaniauskas, *Quasispin and Isospin in the Theory of Atom* (Mokslas, Vilnius, 1984) [in Russian].
- [21] G. Gaigalas and Z. Rudzikas, On the secondly quantized theory of the many-electron atom, J. Phys. B **29**(15), 3303 (1996), <https://doi.org/10.1088/0953-4075/29/15/007>
- [22] G. Gaigalas, Z. Rudzikas, and C. Froese Fischer, An efficient approach for spin-angular integrations in atomic structure calculations, J. Phys. B **30**(17), 3747 (1997), <https://doi.org/10.1088/0953-4075/30/17/006>
- [23] J.P. Grant, *Relativistic Quantum Theory of Atoms and Molecules* (Springer, New York, 2007).
- [24] P. Bogdanovich, G. Gaigalas, A. Momkauskaitė, and Z. Rudzikas, Accounting for admixed configurations in the second order of perturbation theory for complex atoms, Phys. Scr. **56**(3), 230–239 (1997), <https://doi.org/10.1088/0031-8949/56/3/002>
- [25] P. Bogdanovich, G. Gaigalas, and A. Momkauskaitė, Accounting for correlation corrections to interconfigurational matrix elements, Lith. J. Phys. **38**(5), 443–451 (1998) [in Russian].
- [26] C. Froese Fischer, T. Brage, and P. Jönsson, *Computational Atomic Structure: An MCHF Approach* (IoP, Bristol, UK, 1997), <https://doi.org/10.1201/9781315139982>
- [27] G. Gaigalas, The library of subroutines for calculation of matrix elements of two-particle operators for many-electron atoms, Lith. J. Phys. **42**(2), 73–86 (2002).
- [28] C. Froese Fischer, M. Godefroid, T. Brage, P. Jönsson, and G. Gaigalas, Advanced multi-configuration methods for complex atoms: I. Energies and wave functions, J. Phys. B **49**(18), 182004 (2016), <https://doi.org/10.1088/0953-4075/49/18/182004>
- [29] G. Gaigalas, A program library for computing pure spin-angular coefficients for one- and two-particle operators in relativistic atomic theory, Atoms **10**(4), 129 (2022), <https://doi.org/10.3390/atoms10040129>
- [30] G. Gaigalas, O. Scharf, and S. Fritzsche, Maple procedures for the coupling of angular momenta. VIII. Spin-angular coefficients for single-shell configurations, Comput. Phys. Commun. **166**(2), 141–169 (2005), <https://doi.org/10.1016/j.cpc.2004.11.003>
- [31] Y.T. Li, K. Wang, R. Si, M. Godefroid, G. Gaigalas, Ch.Y. Chen, and P. Jönsson, Reducing the computational load – atomic multiconfiguration calculations based on configuration state function generators, Comput. Phys. Commun. **283**, 108562 (2023), <https://doi.org/10.1016/j.cpc.2022.108562>
- [32] L. Kitovienė, G. Gaigalas, P. Rynkun, M. Tanaka, and D. Kato, Theoretical investigation of the Ge isoelectronic sequence, J. Phys. Chem. Ref. Data **53**, 033101 (2024), <https://doi.org/10.1063/5.0187307>
- [33] P. Rynkun, S. Banerjee, G. Gaigalas, M. Tanaka, L. Radžiūtė, and D. Kato, Theoretical investigation of energy levels and transition for Ce IV, A&A **658**, A82 (2022), <https://doi.org/10.1051/0004-6361/202141513>
- [34] G. Gaigalas, P. Rynkun, S. Banerjee, M. Tanaka, D. Kato, and L. Radžiūtė, Theoretical investigation of energy levels and transition for Pr IV, MNRAS **517**, 281 (2022), <https://doi.org/10.1093/mnras/stac2401>
- [35] R.D. Cowan, *The Theory of Atomic Structure and Spectra* (University of California Press, Berkeley, CA, USA, 1981)
- [36] P. Jönsson, X. He, C. Froese Fischer, and I.P. Grant, The GRASP2K relativistic atomic structure package,

Comput. Phys. Commun. **177**, 597–622 (2007),
<https://doi.org/10.1016/j.cpc.2007.06.002>

ANTROSIOS EILĖS RELĖJAUS IR ŠRĘDINGERIO TRIKDYMŲ TEORIJA, SKIRTA GRASP2018 PROGRAMMINIAM PAKETUI: VALENTINĖS–VALENTINĖS KORELIACIJOS

G. Gaigalas, P. Rynkun, L. Kitovienė

Vilniaus universiteto Fizikos fakulteto Teorinės fizikos ir astronomijos institutas, Vilnius, Lietuva

Santrauka

Vienas pagrindinių uždavinių atomo struktūros skaičiavimuose yra tikslus elektronų koreliacijų iškaitymas. Norint atliliki tikslius skaičiavimus, būtina atsižvelgti į įvairių tipų elektronų koreliacijas, o tai dažnai veda prie didelės konfigūracinių būsenų funkcijų (KBF) erdvės. Šiame darbe toliau plėtojamas antrosios eilės trikdymų teorija grįstas metodas, siekiant nustatyti svarbiausias KBF, kurios doro didžiausią įtaką kamieno–valentinėms, kamieno, kamieno–kamieno ir valentinėms–valentinėms koreliacijoms. Šis metodas parentas relatyvinės superpozicijos ir stacionariosios antrosios eilės Relėjaus ir Šredingerio daugelio kūnų trikdymų teorijos nereduotinėje tensorinėje formoje (G. Gaigalas, P. Rynkun, L. Kitovienė, Second-order Rayleigh–Schrödinger perturbation theory for the GRASP2018 package: Core–valence correlations, Lith. J. Phys. **64**(1), 20–39 (2024), <https://doi.org/10.3952/physics.2024.64.1.3>), (G. Gaigalas, P. Rynkun, L. Kitovienė, Second-order Rayleigh–Schrödinger per-

turbation theory for the GRASP2018 package: Core correlations, Lith. J. Phys. **64**(2), 73–81 (2024), <https://doi.org/10.3952/physics.2024.64.2.1>), (G. Gaigalas, P. Rynkun, L. Kitovienė, Second-order Rayleigh–Schrödinger perturbation theory for the GRASP2018 package: Core–core correlations, Lith. J. Phys. **64**(3), 139–161 (2024), <https://doi.org/10.3952/physics.2024.64.3.1>) metodų deriniu. Metodas yra išplėstas norint papildomai įtraukti valentines–valentines koreliacijas. Ši metodą galima taikyti atomo ar jono energijos spektro ir kitų charakteristikų skaičiavimui, esant skirtiniems valentinių sluoksnių pagrindiniam, orbitiniams kvantiniams skaičiams bei užpildymams. O koreliacijos, kurių negalima įtraukti pagal trikdymų teoriją, yra įtraukiamos naudojant išprastą būdą. Sukurtas metodas leidžia žymiai sumažinti KBF erdvę, tai ypač aktualu sudėtingiems atomams ir jonams. Darbe, kaip metodo taikymo pavyzdys, taip pat pateikiama Se III energijos struktūros skaičiavimai.